

University of Alberta

**A CAPACITANCE SENSOR FOR PIPELINE FLOWS OF OIL-WATER
MIXTURES**

By

M M A Sayeed Rushd



A Thesis Submitted To The Faculty Of Graduate Studies And Research In Partial
Fulfillment Of The Requirements For The Degree Of Master Of Science

In

Chemical Engineering

Department Of Chemical And Materials Engineering

Edmonton, Alberta

Fall 2008



Library and
Archives Canada

Bibliothèque et
Archives Canada

Published Heritage
Branch

Direction du
Patrimoine de l'édition

395 Wellington Street
Ottawa ON K1A 0N4
Canada

395, rue Wellington
Ottawa ON K1A 0N4
Canada

Your file *Votre référence*

ISBN: 978-0-494-47403-7

Our file *Notre référence*

ISBN: 978-0-494-47403-7

NOTICE:

The author has granted a non-exclusive license allowing Library and Archives Canada to reproduce, publish, archive, preserve, conserve, communicate to the public by telecommunication or on the Internet, loan, distribute and sell theses worldwide, for commercial or non-commercial purposes, in microform, paper, electronic and/or any other formats.

The author retains copyright ownership and moral rights in this thesis. Neither the thesis nor substantial extracts from it may be printed or otherwise reproduced without the author's permission.

AVIS:

L'auteur a accordé une licence non exclusive permettant à la Bibliothèque et Archives Canada de reproduire, publier, archiver, sauvegarder, conserver, transmettre au public par télécommunication ou par l'Internet, prêter, distribuer et vendre des thèses partout dans le monde, à des fins commerciales ou autres, sur support microforme, papier, électronique et/ou autres formats.

L'auteur conserve la propriété du droit d'auteur et des droits moraux qui protègent cette thèse. Ni la thèse ni des extraits substantiels de celle-ci ne doivent être imprimés ou autrement reproduits sans son autorisation.

In compliance with the Canadian Privacy Act some supporting forms may have been removed from this thesis.

Conformément à la loi canadienne sur la protection de la vie privée, quelques formulaires secondaires ont été enlevés de cette thèse.

While these forms may be included in the document page count, their removal does not represent any loss of content from the thesis.

Bien que ces formulaires aient inclus dans la pagination, il n'y aura aucun contenu manquant.



Canada

ABSTRACT

Lubricated pipe flow (LPF) is a flow regime characterized by a viscous oil core enveloped by a lubricating water annulus. The resulting friction losses are economically lower than those associated with the flow of the viscous oil itself. One of the most significant technical challenges for this technology is flow instability caused by the formation of a wall-coating of viscous oil and thinning and/or loss of the lubricating water layer. This research is intended to test capacitance sensors to quantify both the wall coating- and annular water-layer thicknesses. The responsiveness of such sensors to the involved flow conditions have been investigated with two geometrically different laboratory-scale sensors: a bench-scale concentric pipe-spool set-up and a rectangular flow cell. The experimental results are in good agreement with simulations produced using COMSOL Multiphysics. This research suggests that information about the intended thicknesses in LPF can be reliably obtained using capacitance sensors.

ACKNOWLEDGEMENTS

I would like to thank the Chemical and Materials Engineering Department in the University of Alberta for providing me with financial and logistic support throughout my graduate program. I would also express gratitude to my supervisor, Dr. Sean Sanders for ensuring economic assistance for my work. He deserves more thanks for trusting me to initiate this significant research. I am also thankful to him for his prudent and friendly guidance throughout my graduate studies.

I want to thank two technical personnel to the department of Chemical and Materials Engineering in the University of Alberta for their helping me to construct and operate the experimental setups. Electronics technician Mr. Walter Boddez (Instrument Shop Supervisor) assisted to fix the electrical instruments and machinist technician Mr. Dave Parlin (Machine Shop Technician) helped to construct the apparatus. Without their valuable service it would not be possible for me to conduct the experiments for this research project. I am also grateful to my colleagues for their invaluable moral support.

TABLE OF CONTENTS

1.	INTRODUCTION	1
1.1.	Background	1
1.2.	Objectives	6
1.3.	Research Plan	6
2.	LITERATURE REVIEW	8
2.1.	Pipeline transportation of heavy oil and bitumen	8
2.2.	Lubricated pipe flow	10
2.2.1.	Background	10
2.2.2.	Classification	11
2.2.2.1.	Core Annular Flow	12
2.2.2.2.	Continuous Water Assisted Flow	13
2.2.2.3.	Self Lubricated Flow	13
2.2.3.	Factors Governing Flow Stability	13
2.2.4.	Challenges	18
2.3.	Measurement technologies	19
2.4.	Capacitance	22
2.4.1.	Theoretical study	22
2.4.2.	Capacitance sensors	24
2.4.3.	Dielectric Constants for Emulsions	27
2.5.	Summary	29

3.	APPARATUS AND PROCEDURES	31
3.1.	Apparatus	31
3.1.1.	Cylindrical Capacitor	32
3.1.2.	Pipe Spool Capacitor	32
3.1.3.	Parallel Plate Capacitor	33
3.1.4.	Design Constraints	36
3.2.	Instruments	36
3.2.1.	FLUKE RCL meter	36
3.2.2.	B/W CCD camera	39
3.2.3.	Camcorder	39
3.3.	Procedures	39
3.3.1.	Connecting the Apparatus	39
3.3.2.	Liquid Placement	39
3.3.3.	Using Emulsion	41
4.	SIMULATION	43
4.1.	Introduction	43
4.2.	Model definition	44
4.2.1.	Domain equations	44
4.2.2.	Boundary conditions	45
4.3.	Modeling Using the Graphical User Interface	45
4.3.1.	Model navigator	46
4.3.2.	Geometry modeling	47
4.3.3.	Physics settings	47

4.3.3.1. Boundary conditions	47
4.3.3.2. Subdomain settings	47
4.3.4. Mesh generation	48
4.3.5. Computing solution	50
4.3.6. Post processing and visualization	50
4.3.7. Calculation of Capacitance	51
4.4. Discussion	52
4.4.1. End Effects	52
4.4.2. Meshing	56
5. RESULTS AND DISCUSSION	59
5.1. Capacitance: Air as dielectric fluid	59
5.2. Cylindrical Capacitor	60
5.2.1. Measurement of dielectric constant	60
5.3. Pipe Spool Capacitor	61
5.3.1. Dielectric liquids: Naphtha and water	61
5.3.2. Dielectric liquids: Emulsion and water	66
5.4. Parallel Plate Capacitor (PPC)	69
5.4.1. Dielectric Liquids: Stationary and Flowing Water at Different Temperatures	69
5.4.2. Dielectric Liquids: Bitumen and Water	70
5.5. Summary	77
6. CONCLUSIONS AND RECOMMENDATIONS	79

REFERENCES	84
APPENDICES	
APPENDIX 1: Schematic outlines of experimental capacitors (capacitance sensors)	90
APPENDIX 2: Specifications for modeling CC cell geometry with COMSOL	99
APPENDIX 3: Specifications for modelling geometry with COMSOL for the PPC	100
APPENDIX 4: Capacitance of the sensors with air as dielectric fluid	102
APPENDIX 5: Capacitance of PSC filled with Naphtha (N) and Water (W) at room temperature	103
APPENDIX 6: Capacitance of PSC filled with emulsion (E:E:E) at room temperature	104
APPENDIX 7: Photographs of bitumen with stationary water in parallel plate capacitor	105
APPENDIX 8: Photos for the average thicknesses of bitumen with flowing water	109
APPENDIX 9: Capacitance for water flowing over bitumen in the PPC	111

LIST OF TABLES

Table	Title	Page
2.1	Dependence of capacitance on the phase distribution of dielectrics (Strizzolo et al., 1993)	26
3.1	Design constraints for the sensors	38
4.1	Specifications for modeling geometry with COMSOL for pipe spool capacitor	49
4.2	Relative permittivity of the dielectric media found in the three capacitance sensors studied for the present work	50
4.3	Simulation results demonstrating the impact of end effects on predicting the capacitance of the PPC (without TEFLON boards and with only air as the dielectric fluid)	56
4.4	Simulation results showing the impact of meshing on predicted capacitance of the PPC (without TEFLON board and with only air as dielectric fluid)	57
5.1	Capacitance of the sensors with air as dielectric fluid	60
5.2	Dielectric constants for reference and experimental liquids	62
5.3	Capacitance of PSC with Naphtha (N) and Water (W)	63
5.4	Experimental and simulation results for PSC with emulsion (E) and water (W)	68
5.5	Capacitance of parallel plate capacitor with water flowing at various Reynolds numbers and temperatures	70
5.6	Capacitance of PPC with bitumen layer and stationary water	73

A2	Specifications for modeling CC cell geometry with COMSOL	99
A3	Specifications for modeling geometry with COMSOL for the PPC	100
A4	Capacitance of the sensors with air as dielectric fluid	102
A5	Capacitance of pipe spool capacitor filled with Naphtha (N) and Water (W)	103
A6	Capacitance of pipe spool capacitor (PSC) filled with emulsion (E:E:E) at room temperature	104
A9	Capacitance for water flowing over bitumen in parallel plate capacitor	111

LIST OF FIGURES

Figure	Title	Page
2.1	Increment of pressure for increasing wall fouling with time ((Joseph et al., 1997; Arney et al., 1999)	15
2.2	Illustrations showing lubricated pipe flow (LPF): (A) axisymmetric view and (B) cross sectional view (Joseph et al, 1999; McKibben et al, 2000 a)	16
2.3	Effect of free water fraction on pipeline pressure gradients for SLF of bitumen froth (Diameter of pipe = 25mm, superficial froth velocity = 1.25m/s and total water content = 29%) (Sanders et al., 2004)	17
2.4	Cross section of a two-concave-plate capacitance sensor: D is the diameter of the circle and W is the width of the sensor plate (Abouelwafa et al., 1979 b)	27
3.1	Schematic illustrations: (A) Cylindrical Capacitor (CC), (B) Pipe Spool Capacitor (PSC), (C) Parallel Plate Capacitor (PPC)	35
3.2	FLUKE RCL meter (PM 6306): (A) Front panel, (B) 4 wires test cable with banana plug, (C) Round plug	37
3.3	Schematic flow diagrams for experimental setups: (A) Cylindrical Capacitor (CC)/Pipe Spool Capacitor (PSC), (B) Parallel Plate Capacitor (PPC)	40
4.1	Distribution of electric potential on the external boundaries of the PSC	46
4.2	The distribution of 106211 mesh elements for simulating the PSC	48
4.3	Post processing results for the PSC	51

4.4	Illustration showing the propagation of electric field across the electrodes of the parallel-plate capacitor	53
4.5	Simulation of the PPC without TEFLON boards and with only air as the dielectric fluid in it: (A) without external dielectrics (i.e. without end effects), (B) with external dielectrics (i.e. with end effects)	55
4.6	Impact of meshing on measured capacitance	58
5.1	Simulation results showing the zone in a pipe over which capacitance measurements will change with wall coating thickness	65
5.2	Near-wall region where capacitance measurements are sensitive to dielectric changes	66
5.3	Photographs showing bitumen thickness for stationary tests: (A) 1.5mm, (B) 3.0mm, (C) 5mm, (D) 8.5mm and (E) 10.5mm	72
5.4	Capacitance as a function of bitumen layer thickness in the PPC cell	74
5.5	Photographs showing the thickness of bitumen layers during flow tests	75
5.6	Capacitance for changing thickness of bitumen with respect to time	76
6.1	Schematic of proposed PSC with SS electrode over external SS pipe-spool: (A) Top view and (B) Cut-away side view	83
A1.1	Schematic outline of the cylindrical capacitor (CC): (A) top view of bottom end cap, (B) side view of bottom end cap, (C) outer cylinder, (D) inner cylinder, (E) bottom view of upper end cap, (F) side view of upper end cap, (G) dimensions	91

A1.2	Schematic outline of pipe spool capacitor (PSC): (A) cut-away side view of the cell, (B) cut-away upper view of the cell, (C) cut-away view of three concentric pipe spools, (D) top view of lower end cap, (E) cut-away side view of lower end cap, (F) top view of upper end cap, (G) cut-away side view of upper end cap, (H) front view of the 'electrode', (I) top view of the flushed electrode, (J) dimensions	96
A1.3	Schematic outline of FVPPC: (A) whole set up, (B) the capacitance sensor, (C) upper/lower plate containing electrode, (D) front/rear plate with viewing window, (E) dimensions	98
A7.1	Photographs for average bitumen thickness of 1.5 mm	105
A7.2	Photographs for average bitumen thickness of 3 mm	106
A7.3	Photographs for average bitumen thickness of 5 mm	106
A7.4	Photographs for average bitumen thickness of 8.5 mm	107
A7.5	Photographs for average bitumen thickness of 10.5 mm	108
A8.1	Photographs for average bitumen thickness of 8 mm	109
A8.2	Photographs for average bitumen thickness of 3 mm	110

CHAPTER 1

INTRODUCTION

1.1. BACKGROUND

In response to increasing global energy demand and decreasing supply of conventional petroleum resources, increased production of non-conventional petroleum reserves, like heavy oil and bitumen (oil sands), is forecasted (Saniere et al., 2004). In Western Canada, the production of hydrocarbons from these non-conventional reserves increases almost annually. Available methods for exploiting such deposits in Canada have been categorized as mining and “in-situ” production technologies (Saniere et al., 2004). Open pit mining is used for oil sands deposits located at shallow depths from the surface. The in-situ production methods, such as well-bore steam injection and SAGD (Steam Assisted Gravity Drainage) process, are employed for the bitumen deposited at greater depths. Similar techniques are also applied to extract heavy oil (Bello, 2004). Most of these techniques require the transportation of highly viscous mixtures of oil and water from the production site to a collection facility or processing plant. Pipeline-based transportation methods are often used provided the ‘effective’ viscosity of the oil can be reduced through heating, dilution, partial upgrading or emulsification (Saniere et al., 2004; Bello, 2004). These methods require substantial capital investment and operating costs (Bello, 2004); hence, these pipelining technologies are likely to be less feasible with predicted production increases of heavy oil and bitumen, particularly if the fields are spread out or located far from a source of solvent. An alternative means for similar transportation has been suggested as water-lubricated pipelining of viscous crude oil (Sanders et al., 2004). Depending on the application, this technology has been referred to as core-annular flow

(CAF) (Arney et al., 1996; Joseph et al., 1997; Bensakhria et al., 2004), continuous water assisted flow (CWA) (McKibben et al., 2000 a, b) and self-lubricated flow (SLF) (Neiman et al., 1999; Joseph et al., 1999; Schaan et al., 2002).

The varied descriptions of water-lubricated flows are by no means consistent within the field. Here, the classifications provided by McKibben et al. (2000a), Schaan et al. (2002) and Bello (2004) are followed. Core-annular flow (CAF) refers to pipeline transportation of heavy oil when water is added to lubricate the oil core (Joseph et al., 1997; Bensakhria et al., 2004). Here, a thin annular layer of water is maintained around the oil core to protect it from contact with the pipe wall, i.e. the water annulus acts as a lubricant for the pipeline flow of heavy oil (Sanieri et al., 2004). In other words, formation of a wall-coating (fouling) layer is to be avoided. Since wall shear in horizontal pipeline transportation is balanced by the pump pressure and the major shear is endured by the lubricating water for CAF, the pumping energy requirement for this technology is comparable to that for transporting water alone under similar conditions (Arney et al., 1996; Joseph et al., 1997). Maintenance of CAF in a pipeline requires significant investment to prevent the formation of a stagnant layer of oil on the inner surface of the pipe, i.e. wall fouling (Arney et al., 1996; Bensakhria et al., 2004). Two industrial applications of CAF, one in North America and the other in South America, have been cited in the literature (Nunez et al, 1998; Sanieri et al, 2004).

In contrast to CAF, addition of lubricating water is not essential and formation of a fouling layer of bitumen is inevitable for self-lubricated flow (SLF) (Neiman et al., 1999; Joseph et al., 1999; Schaan et al., 2002; Shook et al., 2002). The 'self-lubricating' designation is typically reserved for flows where the mixture already contains sufficient water to provide lubrication; no external source of water is required. It involves the migration of

water droplets in a viscous water-in-oil emulsion to a region of high shear near the pipe wall; the migrated water droplets consequently coalesce to form a water annulus enveloping the bitumen-rich core, thereby providing frictional pressure drops significantly lower than those for transporting bitumen alone through the pipeline (Nunez et al., 1998; Neiman et al., 1999; Joseph et al., 1999; Schaan et al., 2002; Shook et al., 2002). Realizing the economic advantages of such water lubricated flow, Syncrude Canada Ltd developed and patented a variation of SLF to transport bitumen froth from a remote extraction site to the existing operating plant (Nunez et al., 1998; Joseph et al., 1999; Schaan et al., 2002; Sanders et al., 2004).

Contrary to SLF, continuous water assisted flow (CWA) requires the addition of water to promote the formation of the lubricated flow regime. Similar addition is also required for CAF. The primary difference between CAF and CWA is that, for CWA, no measures are taken to avoid the formation of a wall-fouling layer (Mckibben et al., 2000 a, b). Additionally, sustained commercial operation of CWA has not yet been proven.

These different modes of water lubricated transport technologies for viscous oils (heavy oil and bitumen) can be classified under the general category of Lubricated Pipe Flow (LPF), which generally involves a beneficial flow regime consisting of a water-annulus enveloping the oil-rich core. The benefits of LPF are predominantly dependent on the degree of wall fouling and water available to lubricate the oil-rich core (Sanders et al., 2004).

Cumulative wall fouling is one of the most important technical challenges that impedes the continued commercial development of lubricated pipe flow (LPF); other significant challenges include the prediction of frictional pressure drops for different water contents and bitumen characteristics, and the development of a reliable process for

restarting a pipeline after an unexpected shutdown (Joseph et al., 1999; Schaan et al., 2002; Sanders et al., 2004).

The formation of a fouling layer of viscous oil on the pipe wall for LPF has been suggested to be practically unavoidable (Mckibben et al., 2000 a, b; Schaan et al., 2002; Shook et al., 2002). Such attachment of oil on the pipe wall increases the frictional pressure drops compared to those for transporting water; nevertheless, friction losses for LPF with wall fouling are significantly lower than would be expected for a mixture of viscous oil and water (e.g. bitumen froth) (Sanders et al., 2004). Moreover, the hydrodynamic stability of such water lubricated flow regime is 'robust' enough for a water annulus to lubricate an oil core even if the pipe wall is totally fouled (Arney et al., 1996; Shook et al., 2002). But the increment of wall fouling can upset the stability of the beneficial flow regime in LPF (Arney et al., 1996; Joseph et al., 1997), particularly if the volume fraction of water available to provide lubrication is near the lower limit.

To ensure the stability of lubricated pipe flow (LPF) it is necessary to check the wall fouling and/or the water lubrication in the pipe. For that purpose, the presence of fouling oil and lubricating water is indirectly sensed without disturbing the beneficial flow regime by measuring the pressure drop over a length of the pipe (Shook et al., 2002). An increasing pressure drop indicates the increment of wall fouling and/or decrease of lubricating water (Arney et al, 1996; Shook et al, 2002). Depending on the trend of the change of such pressure measurement, preventive action (e.g. adjusting water addition and/or bulk flow rate) is taken to stabilize the LPF. It can take a significant amount of time to determine the appropriate control action, which can ultimately result in operational complexities and increasing operating costs. This kind of challenge can be more economically addressed by using a sensor which is capable of providing a quicker response

about wall fouling and/or water lubrication. Such quantification could play an important role in designing pipelines for LPF. To date, only a few studies have been done to develop a convenient sensor that can be used to quantify the wall fouling and/or lubricating water in LPF.

In this work, a novel capacitance sensor was tested to check its applicability to quantify the fouling oil and lubricating water layers in LPF. Because such a sensor is non-intrusive, it can be used without disturbing the beneficial flow regime. It is also capable of producing a rapid response for any change in wall fouling or lubricating water layers over a short length of pipe. Three laboratory scale sensors (capacitors) of different geometries were tested. One of these sensors was used to qualitatively study the sensitivity of a capacitance sensor to the presence of fouling oil and/or lubricating water in LPF. Such sensitivity was quantified with simulations produced using COMSOL Multiphysics. Another experimental sensor was primarily used to test the impacts of important process conditions (temperature and flow rate) on the capacitance measurement. This apparatus was also employed to examine the response of a capacitor to the changing thickness of a fouling oil layer. The experimental results were compared with COMSOL simulations. An important parameter (dielectric constant) required for producing simulations with COMSOL Multiphysics was experimentally measured with the third capacitance sensor.

This research suggested that using a capacitance sensor to obtain information about thicknesses and/or presence of the wall fouling and lubricating water layer in LPF has significant potential.

1.2. OBJECTIVES

The objectives of this research are:

- i. To test the ability of a nonintrusive capacitance sensor to measure the thicknesses of the fouling oil- and/or lubricating water-annulus in Lubricated Pipe Flow (LPF);
- ii. To compare numerical simulations and experimental measurements for the capacitance sensors developed here.

1.3. RESEARCH PLAN

To meet the research objectives, the following studies were conducted:

- i. A bench-top capacitance sensor was used to study the impacts of various stationary configurations of different liquids on capacitance measurement. The experimental arrangements of the liquids were comparable to those found in lubricated pipe flow (LPF). This study indicated the sensitivity of such a sensor to the presence of fouling oil and/or lubricating water in LPF.
- ii. A flow-through capacitor cell was employed to test the sensitivity of capacitance measurement to important process conditions (flow rate and temperature) of LPF. The apparatus was also used to examine the response of the sensor with changing bitumen coating thickness. This analysis was intended to test the sensitivity of a capacitance sensor to the thickness of wall fouling in LPF.
- iii. Simulations using COMSOL Multiphysics were developed to predict the capacitance of the sensors used for the present work. Experimental results were compared with these predicted values. COMSOL simulations were also employed to quantify the sensitivity of a capacitance sensor to the presence of fouling oil and/or lubricating water in LPF. Thus, the applicability of COMSOL Multiphysics

in simulating experimental setups was tested. This testing was meant to develop confidence in COMSOL simulations to simulate a capacitance sensor applied for LPF.

- iv. A third capacitance sensor was used to determine an important parameter (dielectric constant) of experimental liquids. This parameter was necessary for COMSOL simulations.

CHAPTER 2

LITERATURE REVIEW

2.1. PIPELINE TRANSPORTATION OF HEAVY OIL AND BITUMEN

Heavy oil and bitumen both are asphaltic, dense and viscous oils. Their characteristics are similar, but the term 'bitumen' typically refers to more dense and viscous oils (Saniere et al., 2004). These viscous oils do not flow easily through pipelines because of the high flow resistance caused by the high viscosity. Such flow resistance must be reduced for economic pipeline transportation of heavy oil and bitumen (Nunez et al., 1998). For that purpose, the following methods are being used at present (Nunez et al., 1998; Pardo et al., 2002; Bello, 2004):

- i) Heating
- ii) Dilution
- iii) Emulsification

Heating the pipeline at short intervals throughout its length is a proven technology for transporting bitumen and heavy oil because the viscosities of these oils decrease drastically with increasing temperature (Nunez et al., 1998; Pardo et al., 2002; Saniere et al., 2004). For designing a typical 'hot-oil' pipeline, various expensive considerations, like pipeline expansion, generation of heat, heat loss, insulation, higher corrosion of pipe material at high temperature, number of pumping and heating stations, etc are required (Nunez et al., 1998; Saniere et al., 2004). Hence, it is usually considered as an 'inconvenient and costly' method (Bello, 2004).

Dilution is a popular technology for facilitating pipeline transportation of heavy oil and bitumen. It involves blending viscous oil with solvent which is a less viscous

hydrocarbon, such as condensate, naphtha, kerosene or light crude (Nunez et al., 1998; Pardo et al., 2002; Saniere et al., 2004). This technology requires availability of solvents at the production site, recovery of solvent at the collection facility and return of the recovered solvent to the production site (Nunez et al., 1998; Pardo et al., 2002). Construction and operation of a solvent recovery unit and twinned pipelines (one to return the recovered solvent to the production site) necessitate additional capital investment and operating cost (Saniere et al., 2004). Moreover, decreasing availability of solvent (diluent) makes the development of alternative technologies for the pipeline transportation of viscous oils, like heavy oil and bitumen (Nunez et al., 1998; Pardo et al., 2002) more critical.

Another method for the pipeline transportation of such viscous oil is emulsification. It is based on the fact that the viscosity of an emulsion with a water-continuous phase, i.e. an oil-in-water (O/W) emulsion, is very low compared to the viscosity of the oil (Nunez et al., 1998; Saniere et al., 2004). As a result, the power required for the pipeline transportation of an O/W emulsion is significantly lower than that required for transporting viscous oil (Nunez et al., 1998; Bensakhria et al., 2004). Emulsification involves some expensive factors, such as surfactants for stabilizing the emulsion, breaking the stabilized emulsion to recover oil, and recovering stabilizer and water at the downstream to recycle back to the production site (Nunez et al., 1998; Saniere et al., 2004). The volume and quality of research conducted to study the formation of emulsions for pipeline transport surpasses the work done to look at effective emulsion breaking technology. Presently, no commercially feasible, well established processes exist (Saniere et al., 2004).

An alternative method to transport viscous oil by pipeline is Lubricated Pipe Flow (LPF). This terminology is used to refer to a general class of water-lubricated pipeline

transportation technologies. It has been considered to include different categorizes of water lubricated pipeline flows of viscous oil, such as core annular flow (CAF), continuous water assisted flow (CWA) and self lubricated flow (SLF). In general, LPF involves a thin water sheath around the oil-rich core and this water annulus acts as a lubricant. Such lubrication results in an economic reduction of the pumping energy required for pipeline transportation of bitumen and heavy oil (Nunez et al., 1998; Joseph et al., 1999; Schaan et al., 2002; Shook et al., 2002; Sanders et al., 2004; Saniere et al., 2004). Three industrial applications of this technology can be cited as follows:

- a) A 38.6 km Shell CAF pipeline in the United States (Joseph et al., 1997; Saniere et al., 2004)
- b) A 55 km CAF pipeline in Venezuela (Saniere et al., 2004)
- c) A 35 km line of Syncrude Ltd with SLF in Canada (Nunez et al., 1998; Joseph et al., 1999)

One of the major challenges in commercial applications of LPF is wall fouling, which can promote flow restriction and the loss of the lubricated flow regime (Arney et al., 1996; Saniere et al., 2004). Research is required to decrease the ‘technological uncertainty’ associated with LPF. Presently, it is this uncertainty that causes companies to select one of the more expensive, more traditional pipeline transport technologies, e.g. solvent addition (dilution).

2.2. LUBRICATED PIPE FLOW

2.2.1. Background

Lubricated Pipe Flow (LPF) refers to the water-lubricated transport of heavy oil or bitumen in pipelines. For such lubrication of viscous oil, a continuous layer of water is

required in the region of high shear near the pipe wall. Since wall shear stresses are balanced by pumping pressures in pipeline transportation, this technology requires pumping energy significantly lower than that required to pump the viscous oil alone at the same process condition (Arney et al., 1996; Joseph et al., 1997; Joseph et al., 1999; Bensakhria et al., 2004; Saniere et al., 2004). This is the major economic incentive for the application of LPF. Moreover, compared to other technologies (such as heating, dilution and emulsification), this technology does not require extensive heating, expensive solvents or emulsion stabilizers, twinned pipelines and additional process units. Hence, LPF has been suggested as an important alternative for pipeline transportation of heavy oil and bitumen (Nunez et al., 1998; Bensakhria et al., 2004).

The terminology Lubricated Pipe Flow (LPF) has been used to represent a variety of water lubricated pipeline transportation of highly viscous oil. The major categories of LPF are Core Annular Flow (CAF), Self Lubricated Flow (SLF) and Continuous Water Assisted flow (CWA). For each of these types specific mechanism has been suggested (Joseph et al., 1997; Joseph et al., 1999; McKibben et al., 2000 a, b). In general, a critical (minimum) flow velocity must be established to attain the beneficial flow regime of water lubricated pipe flow of viscous oil, i.e. a critical shear rate is required for LPF. Each of the different LPF classifications requires a mixture of viscous oil and water. These technologies also involve various degrees of wall fouling. For each process, though, the method by which water is provided differs.

2.2.2. Classification

The following classifications have been introduced based on the work of Bello (2004). However, no widely accepted terminology is available.

2.2.2.1. Core Annular Flow

Core Annular Flow (CAF) usually refers to the lubrication of heavy oil by water in pipeline transportation where the primary objective is to avoid wall fouling at all cost. Wall fouling was not found in CAF for perfectly density-matched phases of oil and water (Charles et al., 1961; Russel et al., 1959). Here, the position of an oil core lubricated by a water annulus in a pipe was considered to be exactly concentric. The concept of such Perfect Core Annular Flow (PCAF) (Joseph et al., 1997) was used for the theoretical modeling in initial studies of CAF (Russel et al., 1959). Practically PCAF with a smooth oil-water interface is an ideal model of CAF, while the Wavy Core Annular Flow (WCAF) (Joseph et al., 1997) characterized by the rippled surface of oil core is similar to experimental observations (Bello, 2004). Wavy interface for the density difference between phases was also suggested in different theoretical studies about CAF (Ooms et al., 1984; Ooms et al., 2003). These studies found the position of oil core to be eccentric in the pipe. It was reported that such eccentricity could cause wall fouling (Bensakhria et al., 2004). In order to avoid wall fouling in CAF, specific steps were tried, such as:

- i) Using an optimum value of water to oil flow rates ratio (Bensakhria et al., 2004)
- ii) Adding water using an annular injector (Bensakhria et al., 2004)
- iii) Coating and/or treating the pipe wall to render it hydrophilic (Arney et al., 1996)
- iv) Introducing oil to a water-filled pipe (Sanders, 2008)

Even when due attention was paid to reduce wall fouling in CAF, the industrial applications involved some degrees of fouling, as reported in previous section (2.2.1 Background).

2.2.2.2. Continuous Water Assisted Flow

Continuous Water Assisted flow (CWA) is similar to CAF in that water is added to the flowing oil in order to obtain water lubricated flow. Significantly, though, no effort is made to avoid wall fouling. While pressure drops are obviously higher for CWA, it can be operated stably at much lower water volume fractions than CAF can. Also, no attention needs to be paid to the method (or location) of water injection and no expensive pipe wall treatment is required (McKibben et al., 2000 a, b).

2.2.2.3. Self Lubricated Flow

In contrast to CAF, self lubricated flow (SLF) does not require the addition of lubricating water; instead a mixture of bitumen and water (e.g. bitumen froth) is pumped through the pipe at, or above, a critical flow velocity to attain a water lubricated flow regime similar to the one involved in CWA. The fact that a minimum flow rate is required suggests that a critical shear stress is necessary for some of the dispersed water in the emulsion to migrate to the region of high shear (Kruka et al., 1977, Neiman et al., 1999; Joseph et al., 1999). The migrated water droplets subsequently coalesce to form a continuous water sheath enveloping the oil-rich core and thereby lubricate the pipe flow of a viscous mixture of oil and water, e.g. bitumen froth (Joseph et al., 1999; Bello, 2004; Sanders et al., 2004). Wall fouling will necessarily occur because the migration of the water droplets leaves a viscous oil layer at the wall of the pipe.

2.2.3. Factors Governing Flow Stability

Core annular flow (CAF) is stable for a range of oil and water flow rates (Charles et al., 1961; Joseph et al, 1997; Bensakhria et al, 2004). A lower critical value of superficial oil

velocity for stable CAF was reported as about 0.1m/s (Charles et al., 1961; Ooms et al., 1984). For self lubricated flow (SLF) of bitumen froth, a critical (minimum) bulk velocity was identified as 0.3m/s (Joseph et al., 1999; Neiman et al., 1999). Again, continuous water assisted flow (CWA) of heavy oil was reported to be achieved above the bulk velocity of 0.5m/s (McKibben et al., 2000 b). Below such critical velocity, usually a stratified flow regime (water in the lower part of the pipe and oil above it) is observed (Ooms et al., 1984; Neiman et al., 1999). The requirement of a minimum velocity indicates that a minimum shear is required to be developed over an emulsion of oil and water for a sustainable LPF.

Sustainability of LPF greatly depends on the degree of wall fouling (Joseph et al., 1997) which was suggested to vary with 'pipeline velocity' (Schaan et al., 2002). For example, under similar process conditions, the coating thickness of bitumen in SLF of bitumen froth was found to increase from 5.5mm to 8.5mm when the superficial froth velocity was reduced from 1.2m/s to 0.6m/s (Schaan et al., 2002). The pipe diameter used for that research was 150mm. Such dependence indicates that flow rate is an important tool to control wall fouling in LPF.

A fouling layer of oil on the pipe wall does not necessarily affect the stability of LPF (Joseph et al., 1997; McKibben et al., 2000 b; Schaan et al., 2002; Shook et al., 2002; Sanders et al., 2004). However, it increases the pressure requirement and an uncontrolled build up of wall fouling can destabilize the beneficial flow regime. Figure 2.1 depicts a situation involving Zuata crude oil (density = 996 kg/m³, viscosity = 115 Pa.s at 25°C). The oil was pumped through a 20cm ID and 1km pipeline, which was located in San Tome, Venezuela (Joseph et al., 1997; Arney et al., 1999). Here, the oil was allowed to accumulate on the pipe wall in LPF. Figure 2.1 shows how the required pressure increased

with the aggregation of wall fouling. This demonstrates the necessity of controlling the degree of wall fouling for sustainable LPF.

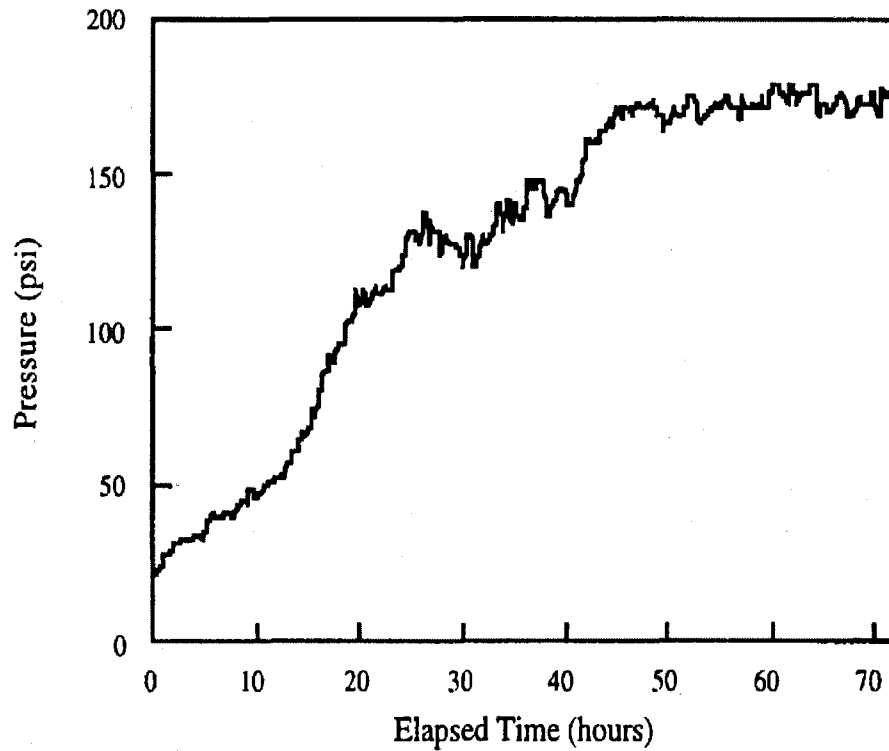


Figure 2.1 Increment of pressure for increasing wall fouling with time (Joseph et al., 1997; Arney et al., 1999)

The beneficial flow regime involved in LPF (with a fouled wall) has been sketched in Figure 2.2. Here, a fouling oil layer is followed by a thin water annulus that lubricates the oil-rich core. The thickness of fouling oil and lubricating water vary depending upon the involved conditions. For example, the thickness of lubricating water layer was measured to vary from 0.17mm to 0.44mm in a 25mm diameter pipe and from 1mm to 7mm in a

600mm diameter pipe with respect to different bulk velocities of bitumen froth (Joseph et al., 1999). Again, at a comparable process condition the thickness of wall fouling was reported to be 2.1mm in a 50mm diameter pipe (Schaan et al., 2002). These values suggest that the wall fouling and lubricating water occupy less than 10% of pipe diameter.

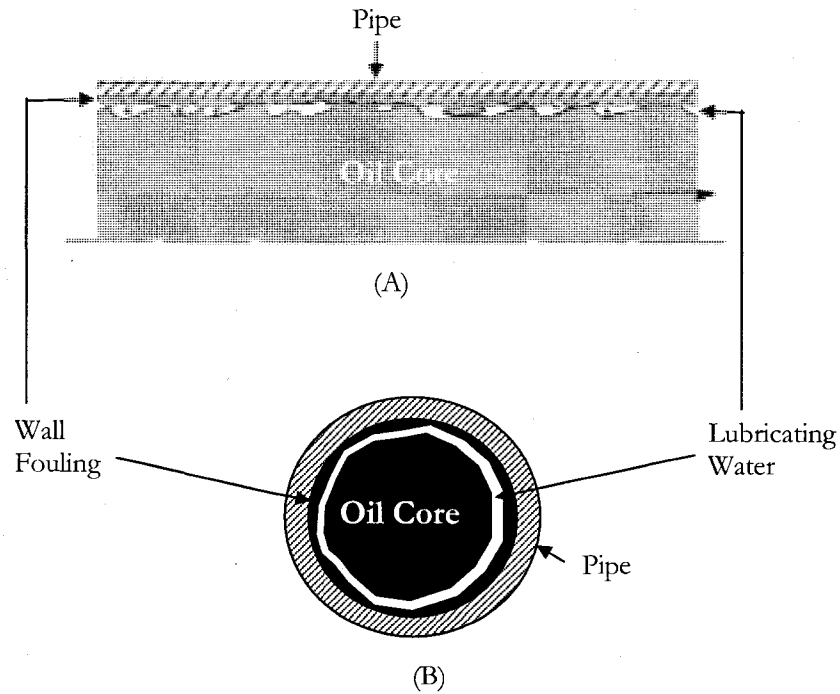


Figure 2.2 Illustrations showing lubricated pipe flow (LPF): (A) axisymmetric view and (B) cross sectional view (Joseph et al, 1999; McKibben et al, 2000 a)

The stability of LPF also depends on the fraction of water in the mixture of oil and water. According to Sanders (2008), this fraction of water is called ‘water cut’. A minimum requirement of ‘water cut’ for lubrication in pipe flows of oil-water mixture was reported to be 0.1 (McKibben et al., 2000 b). However, a lower pressure gradient was experienced for a water fraction of 0.3. For SLF, a part of the total water content of the bitumen froth (‘free

water fraction”) is liberated to form the lubricating water annulus (Shook et al., 2002; Sanders et al., 2004). Such liberation depends on superficial velocity and temperature of the froth. The free water fraction was reported to increase with increasing temperature and to decrease with increasing velocity, given that other flow conditions were fixed (Sanders et al., 2004). The liberated fraction of total water content affects the pressure gradient of SLF. Figure 2.3 demonstrates this effect.

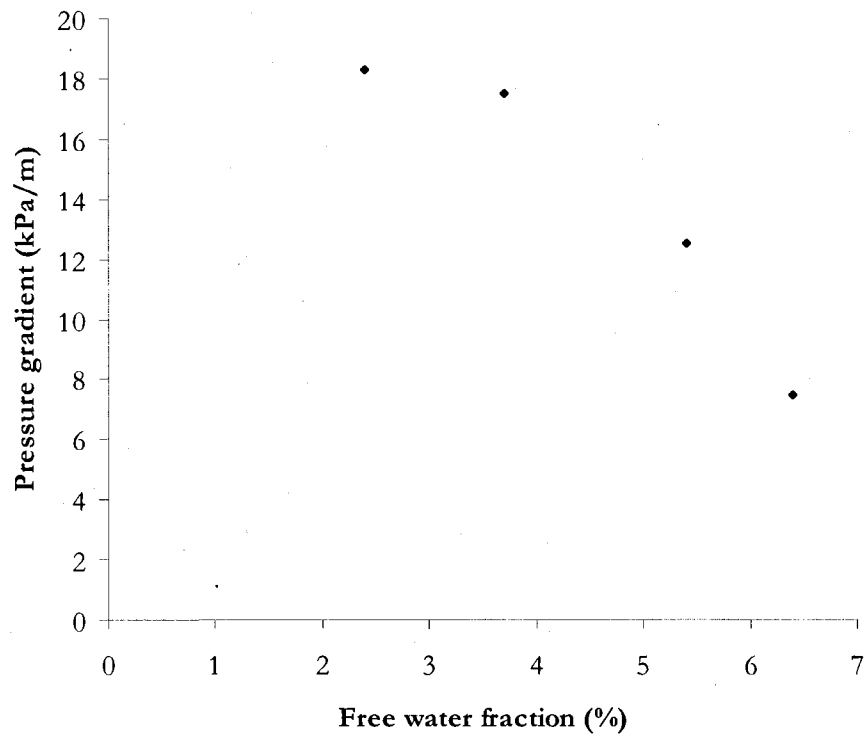


Figure 2.3 Effect of free water fraction on pipeline pressure gradients for SLF of bitumen froth (Diameter of pipe = 25mm, superficial froth velocity = 1.25m/s and total water content = 29%) (Sanders et al., 2004)

2.2.4. Challenges

A number of challenges are involved in expanding the application envelope of lubricated pipe flow (LPF). The major technical challenges can be identified as follows:

- a) Monitoring and controlling wall fouling and water release (Sanders et al., 2004; Schaan et al., 2002)
- b) Designing (scaling up) a water lubricated pipeline as a function of several important parameters, such as pipe diameter, water content, operating temperature and oil properties
- c) Predicting frictional pressure drops for different water content and oil characteristics (Shook et al., 2002; Sanders et al., 2004)
- d) Restarting pipeline after unexpected shutdown (Joseph et al., 1999)

The primary focus of this research is on monitoring wall fouling and water lubrication/release in LPF. This is required for early warnings of flow instability or loss of water lubrication. Such warnings are necessary to prevent loss of lubrication and possible pipeline plugging. For that purpose it is essential to measure the thicknesses of the wall fouling- and/or lubricating water-layer in LPF. Presently, the flow stability during lubricated pipeline operation is evaluated by measuring the pressure drop over a pipe of known length (Sanders, 2008). An increase in the pressure drop is usually related to the increase of wall fouling and/or the decrease of lubricating water (Shook et al., 2002). However, it could also be related to a change in mixture temperature, pipe wall temperature (Schaan et al., 2002) or other unmeasured parameters e.g. oil properties or water chemistry (McKibben et al., 2000 a). For an operating pipeline (such as Syncrude's Aurora Froth Pipeline), it is never clear which interventions an operator should make, such as adjusting the rate of water addition and/or tuning the bulk flow rate. Control of such a

pipeline becomes even more uncertain if the pressure drop is measured over a section of pipe that is many kilometers in length. During this time a significant length of pipe can be over-fouled and this may require restarting the flow system. Thus, a delayed response to increasing wall fouling and/or decreasing mixture water cut can ultimately result in pipeline outages and escalating operating costs.

This challenge in operating lubricated-flow pipelines can be addressed by using a sensor that is capable of yielding real-time information about wall fouling and/or water lubrication. This measurement will also be useful in designing the pipelines, e.g. determining the optimum length to set up pumping stations. To date, very little work has been done to develop a sensor to monitor the wall fouling and/or lubricating water in LPF. In the present work, a novel capacitance sensor has been developed and tested.

2.3. MEASUREMENT TECHNOLOGIES

The major techniques that can be applied to measure the thicknesses of fouling oil- and lubricating water-annulus in LPF are outlined below:

- i. Heat Transfer Measurement: On the basis of measuring the heat transfer coefficients, a method to quantify the fouling bitumen- and lubricating water-layer in LPF was proposed (Schaan et al, 2002). This technology can be efficient for measuring the average thicknesses over a relatively short length (< 1m) of pipe. However, the accuracy of the measurement depends upon knowledge of the thermal conductivity of the wall coating. Implementation of this technology on a commercial scale would be complicated and expensive.
- ii. Optical/Photographic Technique: A photometric method to measure film thickness based on absorption of light passing through a layer of dyed liquid was

described (Mouza et al, 2000). This technique has the characteristics of a good sensor, such as non-intrusiveness, easy calibration, suitability for conducting and non-conducting liquids, capability of measuring very thin films, having high spatial resolution, faster time response and less temperature sensitivity. Unfortunately, it basically depends on the absorption characteristics of the medium, i.e. dyestuff concentration; as a result, it requires optically sensitive dyes and transparent surfaces for the light to pass through. Hence, it is not likely to be applicable for the opaque media like bitumen and heavy oil.

- iii. **Conductance Measurement:** The use of conductance probes for measuring liquid film thickness was addressed in numerous studies (e.g. Coney, 1973). This technology requires a conducting continuous phase and direct contact of the probes with the medium (Bezrodnyy et al, 1992). Since the mixtures involved in LPF consist of a dispersed conducting phase (water) and a continuous non-conducting phase (heavy oil or bitumen), this film thickness measurement technology cannot be utilized for LPF applications.
- iv. **Acoustic Method:** Acoustic sensors are used to measure the thicknesses of liquid films (Bezrodnyy et al., 1992; Kim et al., 2004). For this purpose, a sound wave of known strength is sent through the liquid media from an 'emitter'. Depending on the physical characteristics of the media, the signal loses its strength by a certain amount. This loss can be measured after receiving the emitted wave with a 'receiver'. The measured loss is a direct function of the film thickness. The thicknesses of stagnant and flowing water films on both horizontal and inclined surfaces have been measured with an ultrasonic transducer (Starkovich et al, 1980). Moreover, the ultrasonic technique for film thickness measurements has the

advantages of faster time response, higher mechanical durability and less temperature sensitivity. So, this can be recognized as a potential technology for LPF.

- v. **Capacitance Measurement:** Capacitance sensors have been used to determine the volume fraction in two-phase pipelines (Gregory et al., 1973; Abouelwafa et al., 1979 a, b, 1980; Strizzolo et al., 1993). This technology primarily depends on the permittivity difference between the involved fluids. Since there is a significant difference between the permittivities of the fluids involved in LPF (water ~ 80 , heavy oil or bitumen ~ 2), the potential of a capacitance measurement technique is good. This technology also depends on the spatial distribution of the fluids present in between the electrodes of the sensor (Strizzolo et al., 1993). Again, this ability to sense a change in spatial distribution of the oil and water is important for LPF applications. This signifies the potentiality of capacitance sensors for LPF. Moreover, the principle of operation for such a sensor is well understood and it is relatively straight forward and inexpensive to build such a sensor.

In general, the measurement of capacitance for nonconducting (dielectric) liquids and conductance (resistance) for conducting ones are popular technologies to indirectly sense the respective thicknesses. The unique situation involved in LPF, with the combination of one conducting (water) in another dielectric (oil) liquid has not been widely addressed. Hence, this study focuses on the testing of a capacitance sensor to measure the thickness of the fouling bitumen- and the lubricating water-layer for lubricated pipe flow applications.

2.4. CAPACITANCE

2.4.1. Theoretical Study

The theoretical aspects of capacitance measurement can be typically described from the electrostatic viewpoint (Baxter et al., 1997). From this perspective, capacitance is a measure of the amount of electric charge stored in, for example, two electrodes of a capacitor for an applied electric potential. Similarly, a capacitor is an electric or electronic device that can store electric energy across the insulating materials (dielectrics) placed in between a pair of conducting plates. The process of storing energy in the capacitor involves electric charges of equal magnitude, but opposite polarity, building upon each electrode. The energy stored in a capacitor is equal to the work done to charge it. If the charges on the plates are $+Q$ and $-Q$, and V is the voltage difference between the plates, then the capacitance (C) is given by the following expression:

$$C = \frac{Q}{V} \quad (2.1)$$

The electric charge developed on each plate of a capacitor for an applied voltage depends on the conducting properties of the plates (electrodes) and the dielectric properties of the insulators sandwiched between those. Such insulators are referred to as dielectrics. They are poor conductors of electricity, but efficient supporters of electrostatic fields. A dielectric material helps to store energy, when placed in between the electrodes of a capacitor, by minimizing the flow of current without impeding or interrupting the electrostatic lines of flux. Again, depending on the geometry of a capacitor and the properties of the involved dielectric(s), more specific and convenient equation can be derived to analytically estimate capacitance. For example, to calculate the capacitance (C) of a parallel plate capacitor and a cylindrical capacitor following equations can be used respectively:

$$C = \epsilon_0 \epsilon_r \frac{A}{h} \quad (2.2)$$

$$C = \frac{2\pi\epsilon_0\epsilon_r L}{\ln(b/a)} \quad (2.3)$$

In equations (2.2) and (2.3) ϵ_0 is the permittivity of vacuum (8.85E-12 F/m), ϵ_r is the relative permittivity of the dielectric, A is the surface area (m^2) and h is the distance (m) between the electrodes. In equation (2.3), L is the length of the cylindrical electrodes and b and a are the radii of outer and inner cylinders, respectively. Here, the relative permittivity (dielectric constant) is defined as a number that relates the ability of a material to carry alternating current (ac) to the same ability of vacuum. The dielectric constant of a composite dielectric medium has been found to be a function of the volume fraction of each constituent phase (Gregory et al., 1973; Abouelwafa et al., 1979 a, b, 1980; Strizzolo et al., 1993). Moreover, Strizzolo et al. (1993) have observed that, depending on sensor geometry, the phase distribution in such a composite medium can affect the resultant capacitance. The effect of phase distribution on the capacitance of a parallel plate capacitor is demonstrated in Table 2.1. The simplified analysis of Table 2.1 suggests that capacitances for composite dielectric media with similar volume fraction but spatially different phase distributions are different. Thus, a capacitance measurement can be expected to carry information about the position and volume fraction of each dielectric phase present in the electric field of a capacitance sensor. Again, this effect is also dependent on the geometry of the sensor.

The concept of capacitance can also be described from the molecular perspective (Moullin et al., 1940, 1944). Such descriptions suggest that when a voltage is applied on the plates of a capacitor, one plate carries a surge of electrons (-ve charge) and at the same time

the other plate experiences an equal dearth of electrons (+ve charge). At this point, the strong molecular symmetry (i.e. the symmetric charge distribution) of the (ideal) dielectric does not allow the electrons to pass from one electrode to the other. Thus electric charge is stored in a capacitor. This stored electric charge results in an electric field which tends to distort the molecular symmetry of the dielectric medium. As a result, electric energy is stored in a capacitor. The extent of this storage depends on the relative permittivity which, in turn, depends on the interaction between the electric field and the neutral molecules of the dielectric; hence, capacitance represents a measurement of such molecular interactions. Any change in spatial arrangement of the components in a composite dielectric can be expected to cause a consequential transformation in the molecular network of the medium. This transformation is likely to cause a resultant change in the corresponding capacitance. Therefore, a capacitor can be used as a sensor to sense the spatial distribution of dielectrics in between the sensor plates.

2.4.2. Capacitance Sensors

Generally a capacitance sensor satisfies the following criteria for a thickness measurement technique (Gregory et al., 1973; Abouelwafa et al., 1979 a, b, 1980; Sun et al., 1982; Teyssedou et al., 1999):

- i) Rapid response
- ii) Measurement over a relatively short length
- iii) Non-intrusiveness
- iv) Independence from flow rate
- v) Poor dependence on temperature
- vi) Economic

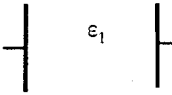
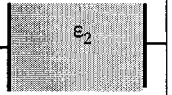
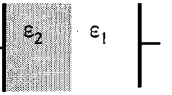
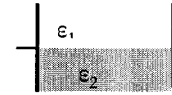
Numerous studies have been done to evaluate the performance of capacitance sensors to measure liquid film thickness in multiphase (gas/liquid) contactors (Dukler et al., 1952; Ogu et al., 1973; Sun et al., 1982). These studies suggest that it is possible to determine the volume fractions in a dielectric ‘composite’ (conducting and/or non-conducting fluids) from the measurement of corresponding capacitance.

Two-phase flows encountered in petroleum industries involve one liquid that is a weak electrolyte (water) present as a dispersed phase and one non-conducting liquid (oil) present as the continuous phase. Thus, a capacitance sensor was employed to continuously monitor the flowing-phase volume fractions in pipelines carrying oil-water mixtures (Gregory et al., 1973). In that study, different capacitor configurations were examined to optimize the geometry for the electrodes. A similar study was done with the intent to construct a sensor with an output (capacitance) varying linearly with volume and relative permittivity of the material within the sensor (Abouelwafa et al., 1980). The theoretical aspects of capacitance sensors with different geometries employed for this study were presented in two different communications (Abouelwafa et al., 1979 a, b). The authors developed geometry-specific empirical equations. For the ‘two-concave-plate’ sensor shown in Figure 2.4, the following empirical equation to estimate the capacitance was suggested (Abouelwafa et al., 1979 b):

$$C = \epsilon_e C_{air} = \epsilon_e \left[\frac{L}{2c_0 \eta_0} \times \left\{ \frac{2W}{D} + 1.393 + 0.667 \ln \left(\frac{2W}{D} + 1.444 \right) \right\} \right] \quad (2.4)$$

In equation (2.4) C is the capacitance with dielectric other than air, C_{air} is the capacitance with air, ϵ_e is the relative permittivity of the involved dielectric, L is the length of the sensor, c_0 ($3E8$ m/s) is the velocity of light in vacuum, η_0 (376.73Ω) is the characteristic impedance of free space, W is the width of the sensor and D is the diameter of the sensor.

Table 2.1 Dependence of capacitance on the phase distribution of dielectrics (Strizzolo et al., 1993)

Case	1	2	3	4
Volume fraction (α)	$\alpha_1 = 1$	$\alpha_2 = 1$	$\alpha_1 = \alpha_2 = 0.5$	$\alpha_1 = \alpha_2 = 0.5$
Ideal configurations of a capacitive sensor				
Analytical capacitance, C_T	$\epsilon_0 \epsilon_1 K$	$\epsilon_0 \epsilon_2 K$	$\epsilon_0 \epsilon_1 K (1 + \epsilon_2 / \epsilon_1) / 2$	$2 \epsilon_0 \epsilon_1 K / (\epsilon_1 / \epsilon_2 + 1)$
<p>A = Surface area of the electrodes</p> <p>h = Distance between the electrodes</p> <p>$K = A/h$</p> <p>ϵ = Dielectric constant</p>				<p>Phase 1: </p> <p>Phase 2: </p>

These studies were focused on evaluation of phase volume fractions in the composite dielectric medium. They did not consider the impact of phase distribution. The significance of phase distribution on measured capacitance was demonstrated by Strizzolo et al. (1993). Their work showed that the analytical capacitance for composite dielectric media (e.g. oil-water mixture) with similar volume fractions, but spatially different phase distributions, is different (see Table 2.1). For identifying the spatial arrangement of different phases in multiphase flows, a novel application of distributed sensor arrays was

proposed (Jaworski et al., 1999; Jaworski et al., 2003; Dyakowski et al., 2005; Meng et al., 2006). This research suggests that capacitance tomography has the ability to identify the phase distribution in a complex multiphase system, provided the continuous phase permittivity is low and each dispersed phase has a permittivity that is different from the continuous phase (and different from each other).

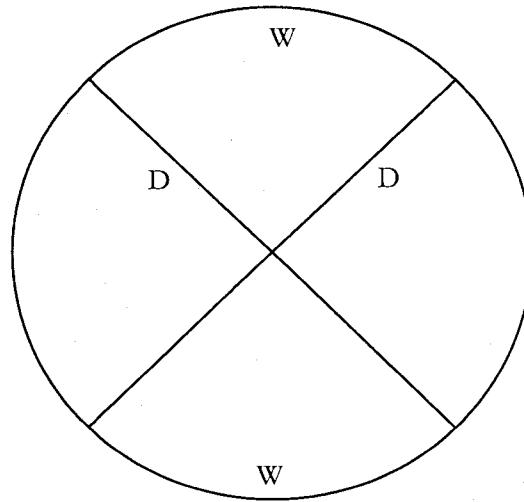


Figure 2.4 Cross section of a two-concave-plate capacitance sensor: D is the diameter of the circle and W is the width of the sensor plate (Abouelwafa et al., 1979 b)

2.4.3. Dielectric Constants for Emulsions

The term 'emulsion' refers to a mixture of two immiscible substances where one substance is dispersed in the other (Bello, 2004). The component with lower volume fraction typically forms the dispersed phase, while the other one with higher volume

fraction constitutes the continuous phase. For example, in a water-in-oil (W/O) emulsion, water is the dispersed phase and the oil forms the continuous phase. The bitumen froth transported using self-lubricated flow is analogous to a W/O emulsion (Sanders et al., 2004).

The effective dielectric constant for a heterogeneous mixture (e.g. water-in-diluted bitumen emulsion) composed of two phases is considered to follow an additive relation with regard to a certain function weighted with each volume fraction (Sherman, 1968). For the mixture (m) of oil (o) and water (w), the relation can be expressed with equation (2.5). The assumption of uniform mixing, like that in emulsions, is implicitly involved with such consideration.

$$f(\epsilon_m) = (1 - \alpha_o)f(\epsilon_w) + \alpha_o f(\epsilon_o) \quad (2.5)$$

In equation (2.5), ϵ and α respectively are dielectric constant and volume fraction, and $f(\epsilon)$ represents a function of ϵ . Various functional forms of $f(\epsilon)$ were described (Sherman, 1968). The most common form is $f(\epsilon) = \epsilon$. Better estimates of ϵ_m were obtained by setting $f(\epsilon) = \ln(\epsilon)$ for water volume fractions up to 60% in a W/O emulsion (Erle et al., 2000). This study has showed that, for water content less than 20%, similar estimates for various forms of $f(\epsilon)$ did not vary appreciably from the experimental results. Thus, equation (2.6) can be used for W/O emulsions (e.g. water-in-diluted bitumen emulsion) with water volume fraction of up to 20%.

$$\epsilon_m = (1 - \alpha_o)\epsilon_w + \alpha_o \epsilon_o \quad (2.6)$$

The present work involves a water-in-diluted bitumen emulsion, where the formation of a stable emulsion with the dispersion of water in bitumen for experimentation is challenging. The stability of such an emulsion most importantly depends on the composition. It was reported that, for naphtha to bitumen (N/B) ratio within 0.5 to 1.5, a

maximum of 35% water could be spontaneously emulsified in diluted (with naphtha) bitumen at room temperature (Yang et al., 2002). Such an emulsion appeared to be stable for an appreciable period and can be used for experimentation. Since the dielectric constants for bitumen and naphtha are typically equal (~ 2), according to equation (2.6) bitumen diluted in naphtha with an N/B ratio of 1 would have a similar relative dielectric constant (~ 2). That is why a water-in-diluted bitumen has been used to simulate the bitumen froth being transported with SLF by Syncrude from their Aurora extraction facilities to the central processing units.

2.5. Summary

A summary of the most relevant and important information taken from the literature review is:

- i. Lubricated Pipe Flow (LPF) has seen limited commercial application thus far because it is viewed as “technically risky”.
- ii. Development of a technique for the online measurement of fouling oil- and lubricating water-layer thickness will facilitate the commercial application of LPF.
- iii. Although capacitance tomography can provide an accurate description of oil/water distribution within a pipe cross-section, the equipment and signal deconvolution algorithms required are quite complex. A simpler capacitance sensor of the type described in this thesis appears to be very promising for systems involving LPF. Clearly, a wall fouling sensor is likely to be simpler and easier to use and more robust than capacitance tomography.
- iv. The capacitance sensor has been used to measure the volume fractions of oil-water mixtures flowing through a pipe.

- v. Capacitance is a function of not only the volume fraction but also the spatial distribution of liquids present in between the electrodes of a capacitor.
- vi. Water-in-diluted bitumen emulsion can be considered to be representative of the bitumen froth.
- vii. For naphtha to bitumen ratio (N/B) 1, less than 20% water can be spontaneously emulsified in bitumen diluted with naphtha.
- viii. The dielectric constant of an emulsion can be determined directly from the volume fractions and dielectric constants of the constituent phases.

CHAPTER 3

APPARATUS AND PROCEDURES

3.1. APPARATUS

For this research three capacitance sensors, namely the Cylindrical Capacitor (CC), the Pipe Spool Capacitor (PSC) and the Parallel Plate Capacitor (PPC), were designed. Each of these had a specific purpose. The CC was developed to measure the dielectric constant of experimental liquids. This parameter was required for COMSOL simulations. As discussed in the following chapters, the simulation results were compared with the experimental results.

The PSC was built and tested to analyze the sensitivity of a capacitance sensor when changing relative positions of various dielectric liquids with respect to the electrodes. This analysis was required to evaluate the sensitivity of a sensor with concave electrodes to the presence of wall fouling- and lubricating water-layer in LPF. Concave electrodes were used for the PSC cell for the following reasons: (i) they are sensitive to phase distributions (Abouelwafa et al., 1979 (b); Strizzolo et al., 1993) and (ii) they would most probably be used for a commercial sensor applied in LPF (Abouelwafa et al, 1980; Gregory et al, 1973). Moreover, the liquid configurations in PSC were representative of the arrangement of fluids that occur during LPF.

The third sensor, PPC, was developed to do experiments with water flowing over a layer of bitumen of known thickness. It was used to evaluate the impact of flow rate on capacitance measurement. It was also used to analyze effect of bitumen coating thickness on measured capacitance. Detailed descriptions of each of these sensors are provided in this chapter.

3.1.1. Cylindrical Capacitor

A schematic outline of Cylindrical Capacitor (CC) is shown here as Figure 3.1 (A) and the detailed specification drawing has been included in Appendix 1 (Figure A1.1). This capacitance sensor was used to determine the dielectric constant of a “pure” liquid or well-mixed emulsion. For such determination, about 60mL liquid was placed in the annulus of the CC. The annular shell was formed by placing two concentric stainless steel (SS) cylinders in between two end caps. The height of each SS cylinder is 152mm. The ID of the outer cylinder is 91mm and the OD of the inner one is 88mm. The TEFLON end caps were grooved to ensure concentric arrangement of the electrodes. The grooves on the lower end cap consisted of o-rings placed beneath the SS cylinders to prevent leakage of liquid from the cell. The upper end cap was not round like the lower one (see Figure A1.1 E and F). It was symmetrically cut off on two sides. This special fabrication of the apparatus ensured facilitation of filling the cell with and evacuating it of the experimental liquids. The SS cylinders acted as the electrodes of the capacitor. Each electrode was connected to a RCL meter (FLUKE, PM 6306).

3.1.2. Pipe Spool Capacitor

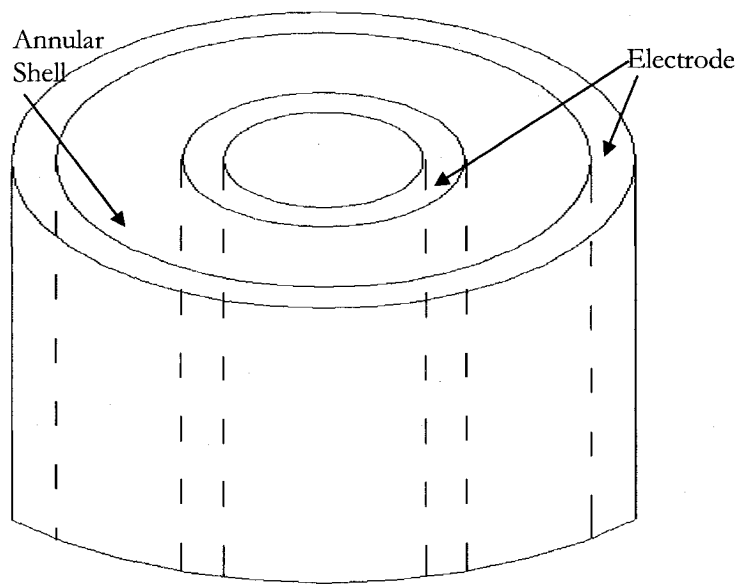
The Pipe Spool Capacitor (PSC) was constructed from PVC. A schematic illustration is shown here as Figure 3.1 (B) and a detailed specification drawing is provided in Appendix 1 (Figure A1.2). The sensor was developed by inserting two 152mm long Stainless Steel (SS) electrodes flush with the inner surface of a 305mm long PVC pipe spool (ID = 63.5mm and OD = 101.6mm). Each electrode was $\frac{1}{4}$ of the pipe’s inner circumference in width and was placed in the middle of the spool as shown in Figures 3.1

(B) and A1.2 (A, B and C). Figure A1.2 (A) shows that the copper screws were fixed to the electrodes so that they could be connected to the RCL meter (FLUKE, PM 6306). The SS electrodes were also surrounded by o-rings to prevent leakage of liquid from the cell. Two more spools were placed inside the outer most pipe-spool to form three concentric shells to place different dielectric liquids. The inner spools were equal in height, but each was smaller in diameter. One of the inner spools had 51.1mm OD and 44.8mm ID, while the other one had 32.4mm OD and 26.0mm ID. Volumes of first, second and central shell of the sensor were about 350 mL, 235 mL and 165 mL respectively. The thickness for each of the first two annuli was 6.1mm and the radius of the shell at the center was 13.0mm. Concentric arrangement of the spools was ensured by placing them in between two grooved end caps. O-rings were placed in the grooves to prevent leakage of liquids from the shells. The end cap placed on top of the cell had holes drilled in five locations so that liquid could be poured into the appropriate shell. The cell was placed in a supporting structure made of nylon. This supporting structure was specially fabricated to make the cell mechanically strong. It helped preventing the leakage of liquid from or within the cell.

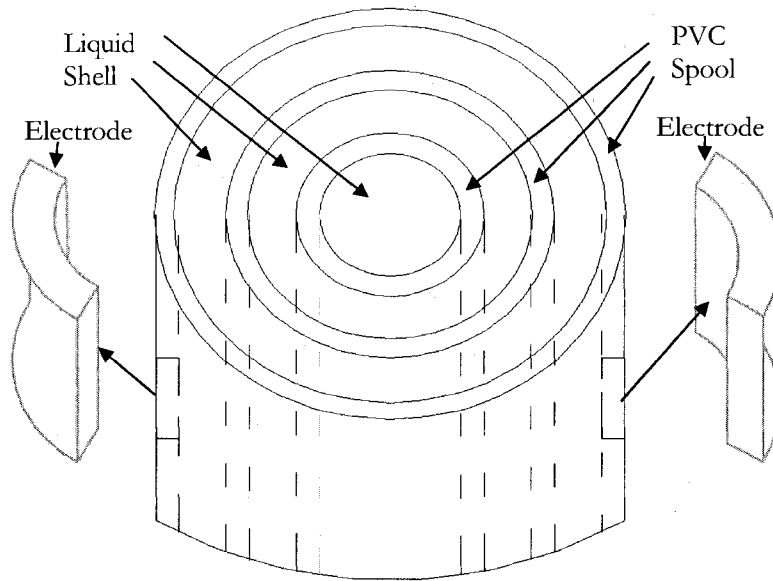
3.1.3. Parallel Plate Capacitor

Figure 3.1 (C) provides an illustration of the Parallel Plate Capacitor (PPC) while a detailed drawing is given in Appendix 1 (Figure A1.3). The rectangular body of the cell was prepared from TEFLON. The upper and lower plates of the cell incorporated two 232cm^2 stainless steel (SS) electrodes placed in parallel. The sensor plates were segregated from the composite dielectric medium comprising (conducting) water and (dielectric) bitumen with TEFLON boards. The electrodes were equipped with copper connecting screws, as shown in Figure A1.3 (A), to connect the cell with the RCL meter (FLUKE, PM 6306). The front

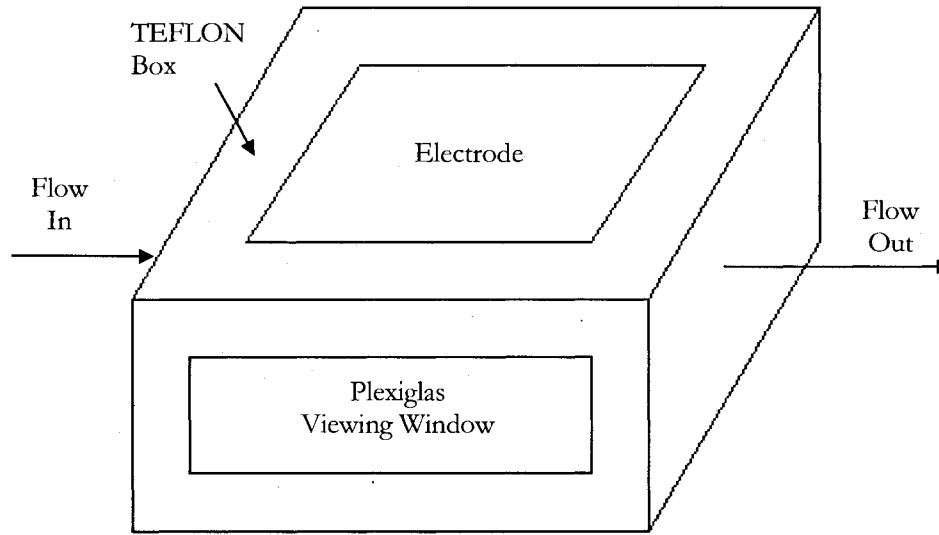
and rear plates of the cell contained two 15mm high and 152mm long Plexiglas viewing windows. O-rings were placed over every part connected to the rectangular TEFLON base to prevent the liquids from leaking out of the cell. The entrance length required to ensure fully developed flow was provided by attaching a 76cm long rectangular PVC channel at the entrance to the cell. A similar 30cm long rectangular conduit was connected at the exit to ensure that water passes out smoothly. Both of the PVC channels were connected to custom-fabricated SS sections to provide smooth transitions from a rectangular channel to a cylindrical pipe. Each joint was flanged properly to prevent leakage of water from the apparatus.



(A)



(B)



(C)

Figure 3.1 Schematic illustrations: (A) Cylindrical Capacitor (CC), (B) Pipe Spool Capacitor (PSC), (C) Parallel Plate Capacitor (PPC)

3.1.4. Design Constraints

Three experimental capacitance sensors were designed based upon the considerations described in Table 3.1.

3.2. INSTRUMENTS

3.2.1. FLUKE RCL Meter

A programmable RCL meter (FLUKE, Model PM 6306) was used to measure capacitance for each of the three sensors described here. A photograph of the FLUKE RCL meter is shown in Figure 3.2 (A). The meter was connected to a computer using a RS-232 interface. The system could be operated from a remote location with a computer having the test software (ComponentView) installed. The software allowed data recording at time intervals as small as one second. The available range for AC test frequency in the RCL meter was from 50Hz to 1MHz and the range for test signal voltage was from 50mV(rms) to 2V(rms). The capacitance was measured at 1MHz and 1V(rms). The high degree of accuracy ($0.1\% \pm 1$ digit) of FLUKE RCL meter allowed recording capacitance in pF with confidence.

To minimize the stray capacitance (unwanted capacitance caused by the connecting wires carrying ac), each experimental sensor was connected to the RCL meter with a 4-wire test cable set having Banana plugs (see Figure 3.2B). This set consisted of coaxial cables with grounded shields. The test cable was attached to the instrument via the round plug, as shown in Figure 3.2 (C), on the front panel and connected to each capacitor by hooking the banana plugs into customized posts fixed with connecting screws on the electrodes. The shortest possible lengths for these connecting posts were used.

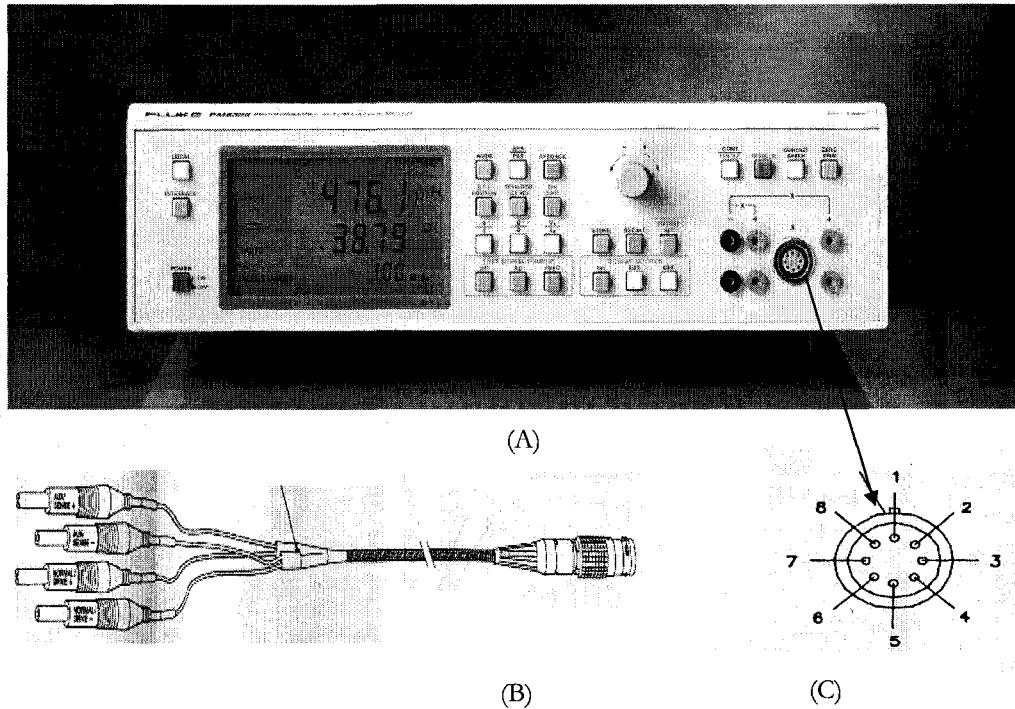


Figure 3.2 FLUKE RCL meter (PM 6306): (A) Front panel, (B) 4 wires test cable with banana plug, (C) Round plug

The capacitance measurement is based on the current and voltage technique (Users manual, 1996). On the basis of the phase angle between test current and voltage, the CPU digitally calculates the equivalent series resistance (R_s), the equivalent series reactance (X_s), and the quality factor ($Q = X_s/R_s$). The microprocessor then determines the dominant parameter depending on the magnitude of Q and the sign of X_s . The RCL meter is able to display various calculated parameters, in addition to the dominant one, within 0.5 second. For the present work, only the capacitance readings were required.

TABLE 3.1 Design constraints for the sensors

Sensor	Design Constraints
Cylindrical Capacitor (CC)	Measuring dielectric constant with reasonable accuracy
	Low infringement of electric field
	Easy addition and recovery of liquid dielectrics
	Requirement of relatively small sample volume
	Easy to clean
	Economic
Pipe Spool Capacitor (PSC)	Concentric arrangement of two liquids in between the electrodes
	Facility to change positions and thicknesses of the liquids with respect to the electrodes
	Maintenance of a distinct boundary between a pair of dielectric liquids
	Prevention of mixing and leaking
	Yielding a minimum capacitance of 1pF
	Mechanically strong
	Simple in construction
	Easy to handle and clean
	Requirement of relatively small sample volume
Economic	
Parallel Plate Capacitor (PPC)	Ability to control bitumen coating thickness
	Simultaneous placement of bitumen and water
	Measuring thickness of bitumen by visual observation
	Measurement of temperature with reasonable accuracy
	Horizontal placement
	Mechanically strong
	Enable flow of tap water under laminar and turbulent conditions
	Requirement of relatively small sample volume
Economic	

3.2.2. B/W CCD Camera

The thickness of bitumen over the lower plate of parallel plate capacitor (PPC) was determined by visual observation through the viewing windows. For that purpose, a B/W CCD camera (Miniature ½" Monochrome Machine Vision Camera, Industrial Vision Source) was used. This camera has a resolution of around 400k pixels and electronic shutter speed from 1/60 to 1/100000 sec. Its zooming power was enhanced by equipping it with a lens (Macro Video Zoom Lens # 18-108, Edmund Optics). As shown in Fig 3.3, it was operated by hooking to the computer with a connecting cord. A 46cm long 15 Watt fluorescent back light was used for this CCD camera.

3.2.3. Camcorder

To record and measure the thickness of bitumen by visual observation through the viewing window of the PPC, a camcorder (Canon Digital Camcorder, MV800) was also used. It was a 800k pixel CCD camera with 20x optical zoom. It required no additional backlight to take photos. It was equipped with a 16MB memory card to store the photographs which could later be transferred to the computer.

3.3. PROCEDURES

3.3.1. Connecting the Apparatus

The basic procedure used to measure capacitance was similar for each sensor. The connections required to record the corresponding capacitance for various arrangements of dielectrics in the sensors have been presented in Figure 3.3. After filling a capacitor with selected liquids, it was connected to the FLUKE RCL meter with proper connecting posts and cables (Banana Plug). For experiments conducted with the parallel plate capacitor

(PPC), it was required to place a camera before one viewing window and, if required, a proper source of light behind the other one. The camera was connected to the computer to store the photographs taken in course of the experiment.

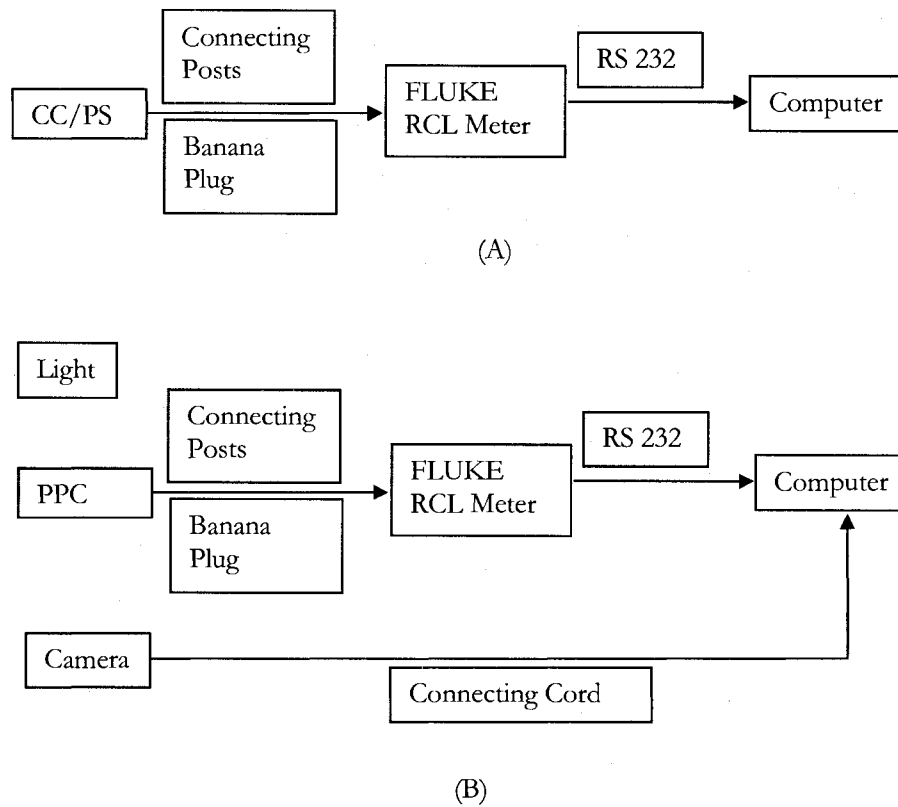


Figure 3.3 Schematic flow diagrams for experimental setups: (A) Cylindrical Capacitor (CC)/Pipe Spool Capacitor (PSC), (B) Parallel Plate Capacitor (PPC)

3.3.2. Liquid Placement

The procedures followed to fill cylindrical capacitor (CC) and pipe spool capacitor (PSC) with dielectric liquids were similar. The required amount of liquid was placed in the CC annulus using a disposable syringe or funnel. Each shell of the PSC was filled in a

similar manner. After capacitance measurements were obtained, the liquids were recovered by siphoning or simply pouring them from the cell.

A layer of bitumen was placed on the lower plate of PPC by removing the plate from the cell and placing it on custom-built stand. The height of each leg was then adjusted to ensure horizontal positioning of the plate. Bitumen was then poured over the horizontal plate to form a layer of nearly-uniform thickness. After reattaching the bitumen-covered plate, layers of paraffin wax were added at the cell entrance and exit to help stabilize the bitumen coating. If the paraffin wax was not used, the bitumen layer was more easily displaced from the lower PPC plate. The cell was then filled with water by opening the inlet valve. Flow of water through the cell was controlled using the inlet valve. The flow rate was measured by weighing the water collected from the discharge over a certain amount of time. The temperature was noted from the thermometers located at the flow cell inlet and discharge.

3.3.3. Using Emulsion

As mentioned in previous chapter, an emulsion of water-in-diluted bitumen (in naphtha) was used for the present work. To prepare this emulsion, an equal volume (about 425 mL) of bitumen and naphtha was transferred to a 1.5L bottle. About 150 mL water was then added to ensure that the water content of the emulsion would be approximately 15%. The bottle was then sealed and shaken for about 1 minute to prepare a stable emulsion (Yang et al., 2002). The emulsion (E) was poured in the first shell of pipe spool capacitor (PSC) with a funnel and other two shells were filled with tap water (W) to obtain the capacitance reading for the E:W:W configuration in the cell. Water was then siphoned out and replaced with emulsion. Thus capacitance readings for E:E:W and E:W:E were

recorded. Once the E:E:E measurements were obtained, the emulsion was recovered by slowly pouring the emulsion from the cell. The emulsion was then returned to the initial mixing bottle. This process was repeated more than thirty times in course of the experiment to check repeatability of the experimental results. After repeating this process for more than ten times, the emulsion was poured in the cylindrical capacitor (CC) to measure its dielectric constant. Before pouring the emulsion into one of the cells, the bottle containing the emulsion was shaken for at least 30 seconds to ensure the uniform dispersion of water.

Chapter 4

SIMULATION

4.1. INTRODUCTION

Every experimental result obtained using each of the three experimental capacitors, namely Cylindrical Capacitor (CC), Pipe Spool Capacitor (PSC) and Parallel Plate Capacitor (PPC), was simulated with COMSOL Multiphysics 3.3a. These simulations were required for the following reasons:

- i) No convincing analytic expressions were found for estimating the capacitance of the PSC sensor.
- ii) Traditional analytic expressions neglect the impact of end effects (discussed later) on measured capacitance. Thus, expressions available for the CC and PPC should be expected to provide poor agreement with the experimental findings.

With the application of COMSOL simulation, it was possible to theoretically estimate the capacitance of the PSC cell. Moreover, this also allowed us to take the impact of end effect in to account in estimating capacitance for all of these sensors. This has yielded better agreement between the experimental and theoretical results.

The following description of the COMSOL simulations used for the present work is based on the examples available in the Model Library of COMSOL Multiphysics 3.3a.

4.2. MODEL DEFINITION

The simulations were prepared using the 3D Electrostatics mode in the Electromagnetics sub-section of the COMSOL Multiphysics Module. The capacitance was calculated on the basis of a postprocessing variable, Electrical Energy Density, as described below.

4.2.1. Domain Equations

The capacitance of a capacitor can be estimated with COMSOL according to the following scheme (Model Library, COMSOL Multiphysics 3.3a):

- i. Capacitance (C) can be defined with respect to the energy of electrostatic field (W) and potential difference (V) in between the electrodes, according to the following expression:

$$C = \frac{2W}{V^2} \quad (4.1)$$

- ii. By specifying the gradient of the electric potential (V), permittivity of free space (ϵ_0) and the relative permittivity (ϵ_r) of the dielectric medium, it is possible to solve Poisson's equation for space charge density (ρ):

$$-\nabla \cdot (\epsilon_0 \epsilon_r \nabla V) = \rho \quad (4.2)$$

- iii. Electrical field (\mathbf{E}) and electric displacement (\mathbf{D}) vectors can be defined according to the expressions:

$$\mathbf{E} = -\nabla V \quad (4.3)$$

$$\mathbf{D} = \epsilon_0 \epsilon_r \mathbf{E} \quad (4.4)$$

- iv. Determining \mathbf{E} and \mathbf{D} from equations (4.3) and (4.4) respectively, W can be calculated by integrating the following:

$$W = \int_{\Omega} \mathbf{D} \cdot \mathbf{E} dV \quad (4.5)$$

- v. From the knowledge of W and V , C can be calculated according to equation (4.1)

4.2.2. Boundary Conditions

The potential boundary conditions were applied to the sensor-plates (electrodes). For one electrode, the boundary condition of **Electric potential** ($V = V_0$) with 1V (V_0) was applied and the other electrode was kept at **Ground** ($V = 0$) potential to simulate a 1 V(rms) potential gradient across the electrodes. For simulating a non-conducting object, it is recommended in the Model Library of COMSOL Multiphysics 3.3a to use **Zero charge/Symmetry** ($\mathbf{n} \cdot \mathbf{D} = 0$) as a boundary condition, and the dielectrics external to the experimental capacitors were mainly composed of different insulating materials; hence, the other external boundaries were maintained at **Zero charge/Symmetry** ($\mathbf{n} \cdot \mathbf{D} = 0$) to simulate the dielectrics surrounding the capacitors. To represent the natural propagation of electric field, the default boundary condition of **Continuity** ($\mathbf{n} \cdot (\mathbf{D}_1 - \mathbf{D}_2) = 0$) was maintained for the internal boundaries. An example of boundary conditions for a simulation of PSC has been included in Figure 4.1. Here, only the voltage distribution on the external boundaries has been depicted.

4.3. MODELING USING THE GRAPHICAL USER INTERFACE

The scheme necessary for modeling the experimental capacitors using graphical user interface in COMSOL has been outlined as follows (Model Library, COMSOL Multiphysics 3.3a). For this description the example of the PSC has been used.

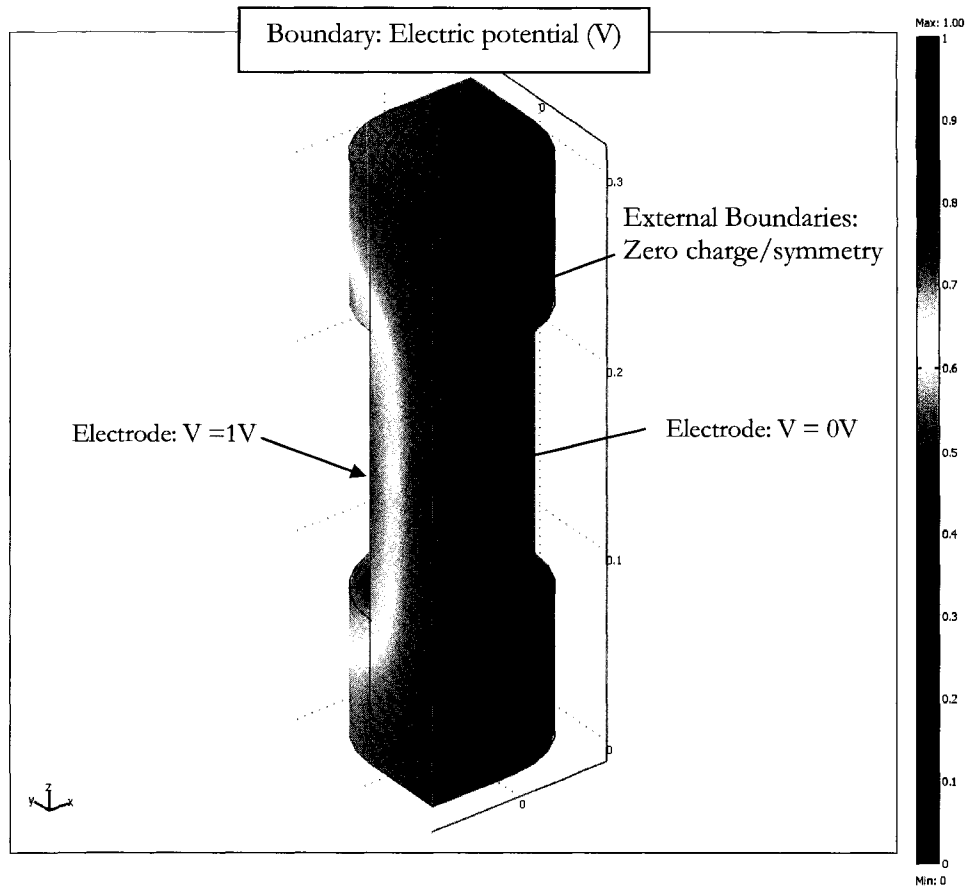


Figure 4.1 Distribution of electric potential on the external boundaries of the PSC

4.3.1. Model Navigator

- i. At first **3D** in the **Space dimension** list was selected.
- ii. Then, in the list of application modes, **COMSOL Multiphysics>Electromagnetics>Electrostatics** was selected.
- iii. Finally **OK** was clicked to confirm the selection.

4.3.2. Geometry Modeling

- i. Required **Blocks & Cylinders** with dimensions as outlined in Table 4.1 were drawn for modeling the PSC. The dimensions for the CC and PSC have been included in appendices 2 and 3.
- ii. All geometric objects were selected using the **Select All** command from the **Edit** menu, and then the **Create Composite Object** dialog box was opened. Finally **OK** was clicked to create a composite object as the union of all objects.

4.3.3. Physics Settings

4.3.3.1. Boundary Conditions

- i. The boundary condition of **Ground** was fixed for one of the boundaries representing the inner surface of an electrode of the capacitor and 1V positive potential for the other one.
- ii. **Zero charge/Symmetry** was selected for the exterior boundaries.
- iii. All of the interior boundaries were set at the boundary condition of **Continuity**. An example of the propagation of voltage over the external boundaries in simulating the PSC with only air has been depicted in Figure 4.1.

4.3.3.2. Subdomain Settings

- i. For the **Constitutive relation**, $\mathbf{D} = \epsilon_0 \epsilon_r \mathbf{E}$, the appropriate dielectric constant (ϵ_r) was selected (see Table 4.2) for each subdomain. For the PSC the major dielectrics were PVC, naphtha, emulsion and water. Dielectric constants of most of the liquids used for the present work were experimentally determined with the CC.

The same parameters for other constitutive dielectrics were taken from the literature, as outlined in Table 4.2.

4.3.4. Mesh Generation

- i. **Initialize Mesh** on the Main toolbar was clicked to create meshes.
- ii. **Refine Mesh**, if required, was clicked on the Main toolbar to create a finer mesh distribution. For example, the refined mesh (mesh elements: 106211) for the PSC has been included in Figure 4.2.

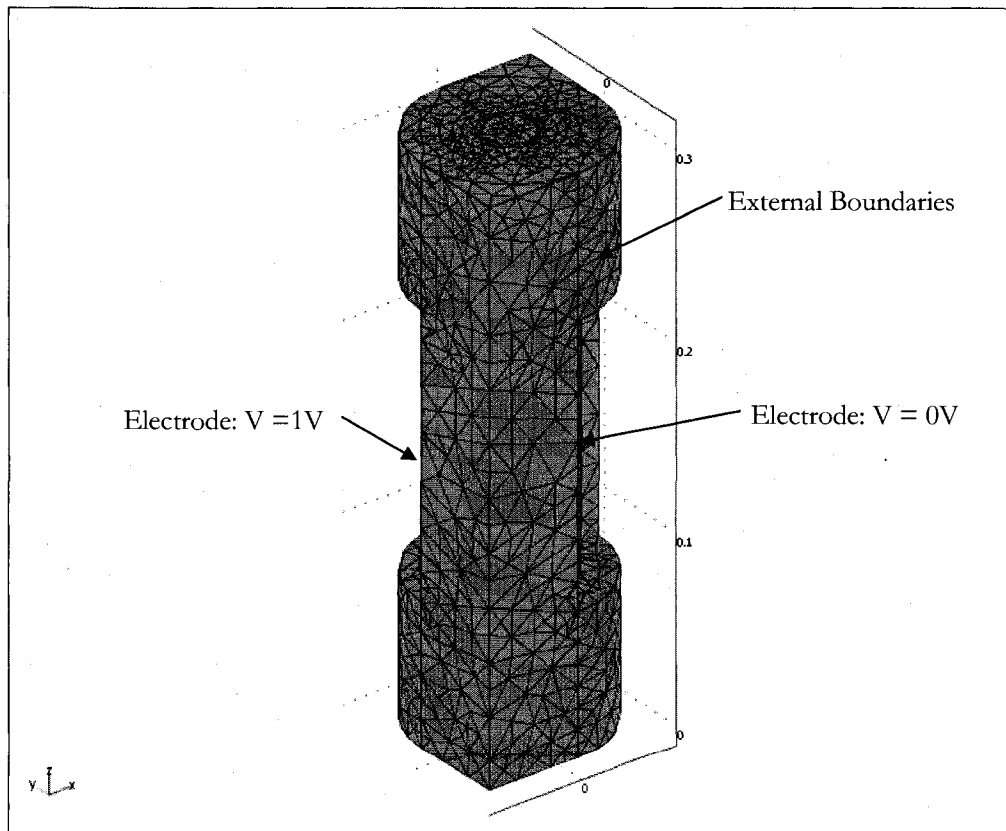


Figure 4.2 The distribution of 106211 mesh elements for simulating the PSC

Table 4.1: Specifications for modeling geometry with COMSOL for pipe spool capacitor

Block	Length (m)			Axis base point			Subject
	X	Y	Z	x	y	z	
BLK1	0.05	0.05	0.3048	0	0	0	Divide the cylinders simulating the pipe spools into four equal parts
BLK2				-0.05	-0.05		
Cylinder	Cylinder parameters (m)		Axis base point			Subject	
	Radius	Height	x	y	z		
CYL1	0.050	0.3048	0	0	0	Outer most pipe spool consisting of the electrodes	
CYL3	0.032					First annular shell adjacent to the electrodes	
CYL5	0.026					First pipe spool in the capacitor placed across the electrodes	
CYL6	0.022					Second annular shell next to the electrodes	
CYL7	0.016					Second pipe spool in the capacitor placed across the electrodes	
CYL8	0.013					Inner most cylindrical shell in the capacitor	
CYL2	0.050	0.1524	0.0762			Hollows in the outer most pipe spool consisting of the flushed electrodes	
CYL4	0.032					Flushed surfaces of the electrodes at 1V(rms) voltage gradient	

4.3.5. Computing the Solution

- i. **Solve** button on the Main toolbar was clicked to compute the solution.

Table 4.2 Relative permittivity of the dielectric media found in the three capacitance sensors studied for the present work

Dielectric	Relative permittivity, ϵ, (isotropic)	Source
Air	1	Perry et al, 1997
TEFLON	2	Lide, 2007 - 2008
Plexiglas	3	
PVC	3	
Naphtha	2	Experiment
Bitumen	2	
Water	80	Perry et al, 1997
Emulsion	8	Experiment
	6-14*	Equation (2.6)

*Based on the actual range of water volume fractions observed during experimentation.

4.3.6. Post Processing and Visualization

- i. The **Plot Parameter** dialogue box was opened from **Postprocessing** tab on the Main toolbar to check **Edge**, **Arrow** and **Streamline** as **Plot type** in **General** tab to view the voltage distribution over the boundaries and the electric field in the composite medium. For example, the post processing result for the PSC has been depicted in Figure 4.3.

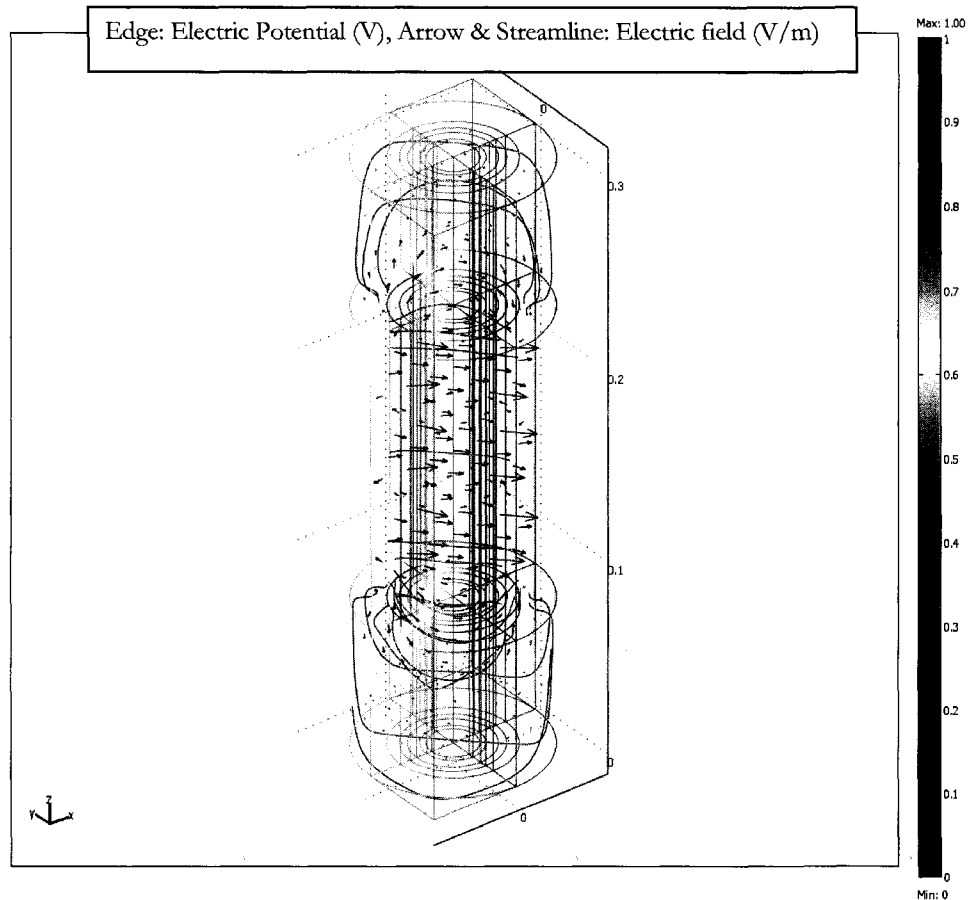


Figure 4.3 Post processing results for the PSC

4.3.7. Calculation of Capacitance

- i. **Subdomain Integration** from **Postprocessing** on the Main toolbar was opened.
- ii. All of the subdomains in the **Subdomain Integration** dialogue box and **Electric energy density** as the **Predefined quantities** were selected for the **Expression to integrate**.
- iii. **OK** was clicked for integration.

- iv. The **Value of integral** in joule (J) was multiplied with 2 to obtain the capacitance (in Farads) because a potential difference of 1V had been fixed between the electrodes for each simulation (see equation (4.1)). The capacitance of the PSC with only air was calculated to be 4pF (see Table 5.1).

4.4. Discussion

The experimental results and corresponding COMSOL simulations are presented in Chapter 5. Here, some important features of the COMSOL simulations are discussed.

4.4.1. End Effects

For a real capacitor, the electric field is uniformly distributed in the central portion of the cell, but at its edges, the field is nonuniform or fringed (Baxter et al, 1997). The effect of fringing electric field on the capacitance is called the end effect. Figure 4.4 depicts the propagation of an electric field between the two electrodes of a parallel plate capacitor. Figure 4.3 depicts the similar propagation for the PSC. The end effects become significant with the increasing distance between the electrodes. As a result, dielectrics present around the capacitor can contribute to the measured capacitance. Though the end effects are neglected in the derivation of the analytic equations (e.g. equations 2.2 and 2.3), it is possible to take the effect into account by solving differential equations (e.g. equations 4.2, 4.3 and 4.4) to estimate capacitance on the basis of an integral (e.g. equation 4.5) according to the Finite Element Method.

In this section, the impacts of end effects on the PPC at a specific condition are described. Similar descriptions for the other two experimental pieces are not provided here. For simplicity, the PPC was simulated without the TEFLON boards on the sensor plates,

i.e. with only air in between the electrodes. Table 4.3 presents the relevant results and Figure 4.5 includes the post processing outcomes of the simulations with and without end effects. Similar results, though have not been reported here, were obtained for simulating the PPC with TEFLON boards in it and also for the PSC and the CC. These results are important to prove the significance of fringing electric field in predicting capacitance of a particular capacitor. On the basis of these simulation results, the following points can be deduced:

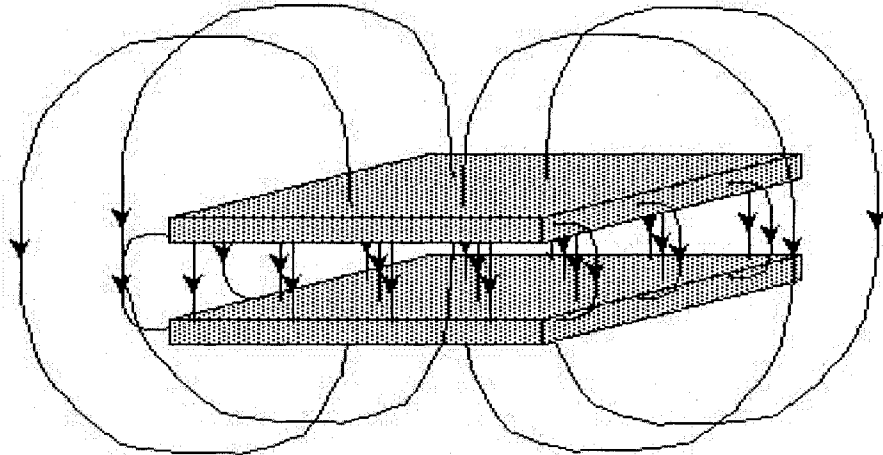
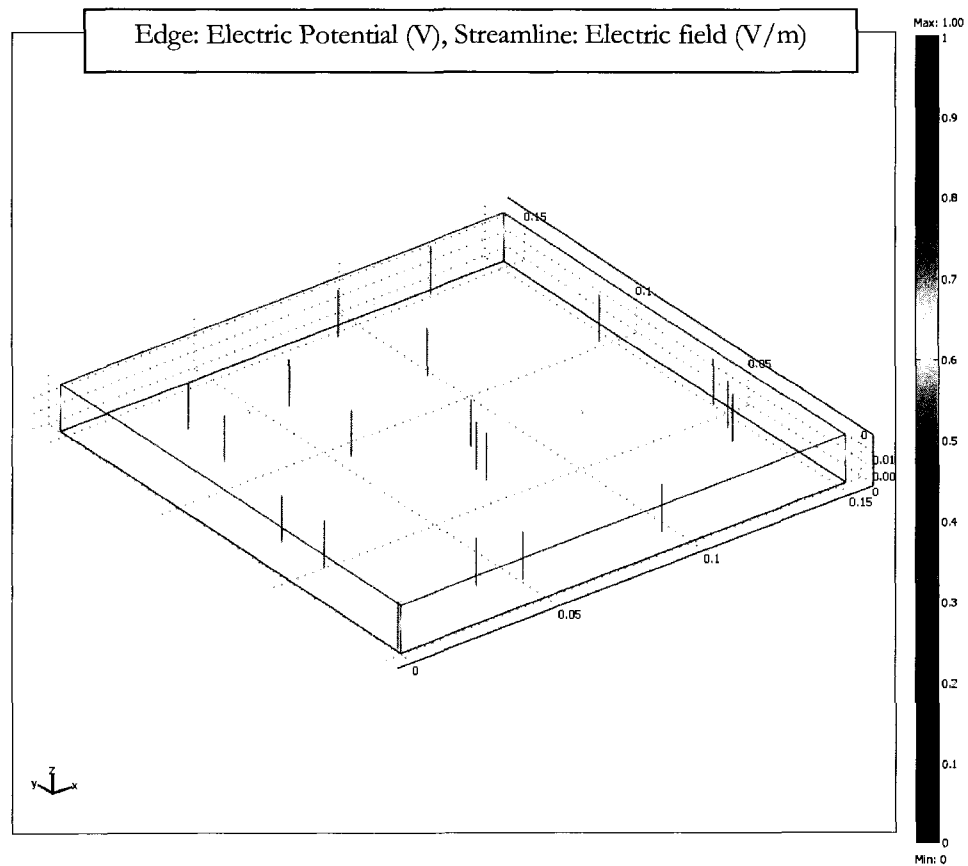


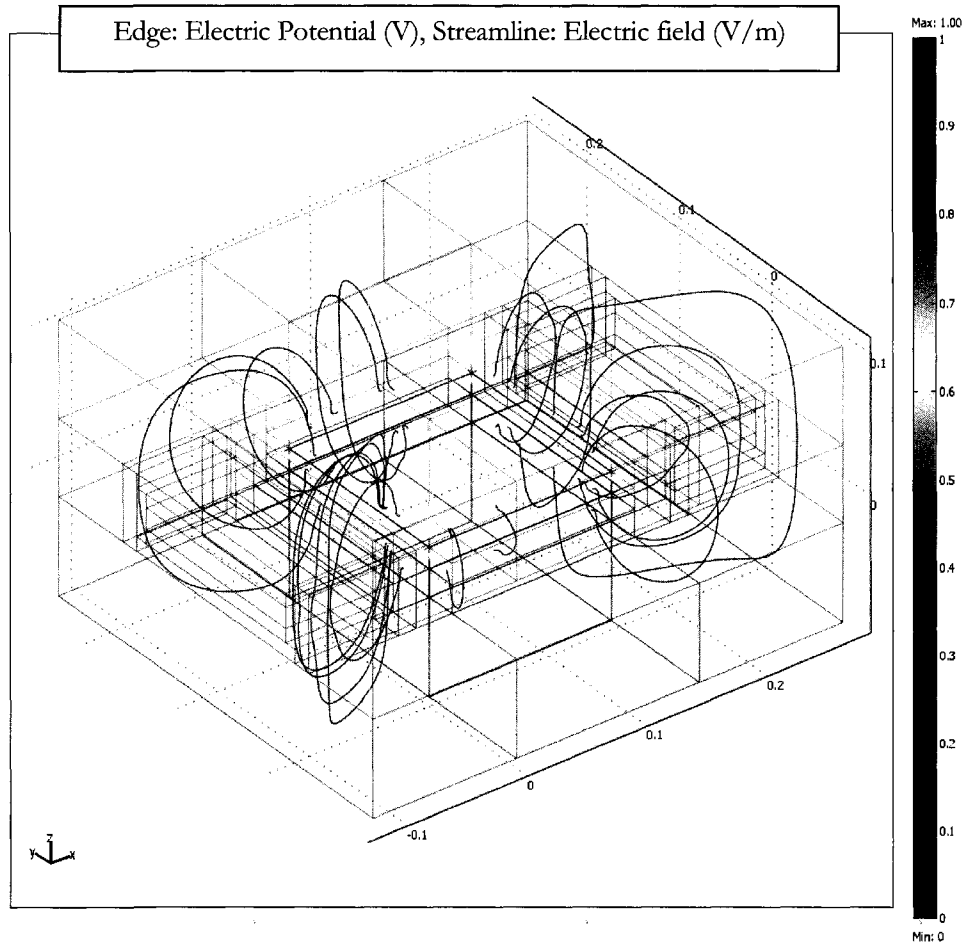
Figure 4.4 Illustration showing the propagation of electric field across the electrodes of the parallel-plate capacitor

- i) Infringing electric fields and dielectrics surrounding the sensor plates were the major contributors to additional capacitance compared to the analytic result.

- ii) Due to uncontrolled end effects, fringing electrostatic field could penetrate the dielectrics making the experimental setup to travel through the surrounding air; so taking the air covering the cell in to account improved the simulations.
- iii) It was required to optimize the dimensions of the external dielectrics to be included in the geometric modeling. In other words, the dielectrics present beyond a particular distance from the sensor plates did not have any significant impact on the predicted capacitance values.



(A)



(B)

Figure 4.5 Simulation of the PPC without TEFLON boards and with only air as the dielectric fluid in it: (A) without external dielectrics (i.e. without end effects), (B) with external dielectrics (i.e. with end effects)

Thus, the dimensions for the external dielectrics were optimized to produce a robust simulation which could be used to simulate the capacitance sensors tested here, namely PPC, PSC and CC. It should be noted that incorporation of the air surrounding the cells was not required in modeling the later two capacitors. The analysis of the simulation

results for three capacitors showed the end effects to be highly dependent on the geometry of each of the three cells.

Table 4.3 Simulation results demonstrating the impact of end effects on predicting the capacitance of the PPC (without TEFLON boards and with only air as the dielectric fluid)

Condition	Capacitance (pF)
Analytic result (Eq 2.2)	14
Simulation without external dielectrics	
Simulation with external dielectrics surrounding the sensor plates	19
Experimental measurement	19

4.4.2. Meshing

The predicted capacitance values were not found to be highly dependent on meshing. Table 4.4 represents the predicted capacitance with respect to the different number of mesh elements for simulations of the PPC, with and without external dielectrics. For this simulation, as stated in previous section, no TEFLON board and presence of only air in the cell were considered. The simulation without external dielectrics represents the condition of the capacitor without the end effects, while the other one signifies the optimized situation with infringing electric field and external dielectrics.

The results presented in Table 4.4 have been plotted with respect to the inverse of mesh # in Figure 4.6. The figure shows that the estimated capacitance for the simulation without external dielectrics (i.e. without the infringement of electric field) is completely independent of meshing and the estimation is equal to the analytic result. This result

validates the fact that the analytic equation is appropriate only when end effects can be ignored. The figure also presents that simulations that consider the external dielectrics (i.e. fringing electric field) have a minor dependency on meshing. The variation in results for mesh-elements above 50,000 is almost negligible. Thus, mesh numbers of 50,000 or greater were considered to be acceptable for the present work. Although the results are not presented here, a similar consideration was found to be applicable to simulate the PPC with TEFLON board and other two cells (PSC and CC).

Table 4.4 Simulation results showing the impact of meshing on predicted capacitance of the PPC (without TEFLON board and with only air as dielectric fluid)

Condition	Mesh-elements (#)	Capacitance, C (pF)
Analytic result (Eq 2.2)	-	
No external dielectrics	18 095	14
	55 865	
	173 236	
External dielectrics	12 440	21
	47 466	20
	152 970	19
Experimental result	-	19

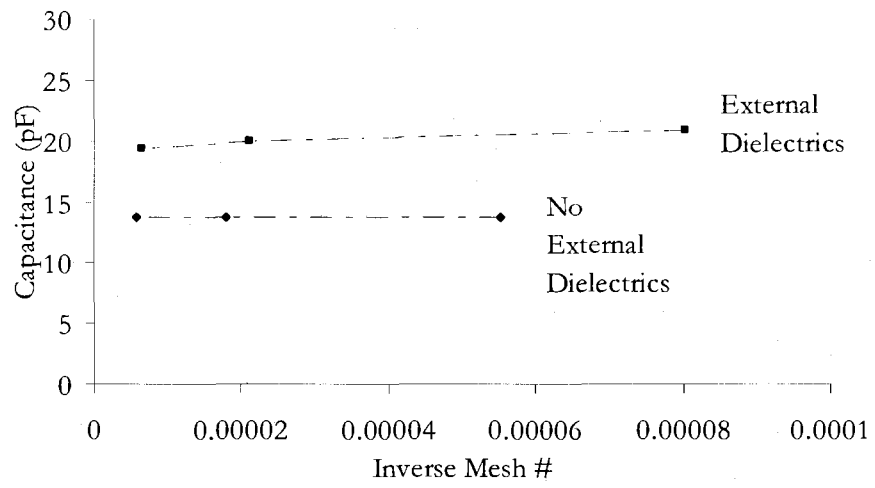


Figure 4.6 Impact of meshing on measured capacitance

Chapter 5

RESULTS AND DISCUSSION

5.1. CAPACITANCE: AIR AS DIELECTRIC FLUID

For each of the test cells described previously, capacitance measurements were obtained using air as the dielectric fluid. This set of experiments was necessary to verify the performance of each cell. The experimental results, analytic estimates and simulation outcomes are presented in Table 5.1. Analytic estimates were based on equations (2.2), (2.3) and (2.4) as described in Chapter 2. These equations do not consider the impact of fringing electric fields and dielectrics external to the capacitor, i.e. the end effects. The lower values of the analytical estimates (see Table 5.1) with respect to the experimental measurements show the importance of considering end effects. For that purpose, every experimental result was simulated with COMSOL Multiphysics 3.3a. The detailed procedure for such simulation is available in Chapter 4. The good agreement between the results from simulation and experiment, as shown in Table 5.1, can be considered as validation of the experimental findings. Similar experimental results recorded at different times in course of the experimentation, along with average and standard deviation of the data, are presented in Appendix 4. Negligible standard deviations with respect to the mean values shown in Table 5.1 indicate that these results are both representative and reproducible.

Table 5.1 Capacitance of the sensors with air as dielectric fluid

Capacitor	Capacitance (pF)			Ratio	
	Analytic (A)	Simulation (S)	Experiment (E)	(S/E)	(A/E)
Cylindrical Capacitor (CC)	249	291	291	1.0	0.9
Pipe Spool Capacitor (PSC)	3	4	4	1.0	0.8
Parallel Plate Capacitor (PPC)	14	16	17	0.9	0.8

5.2. CYLINDRICAL CAPACITOR

5.2.1. Measurement of Dielectric Constants

The dielectric constant is an important parameter for COMSOL simulation and it was necessary to determine this parameter for the liquids used in the present work. For this purpose the Cylindrical Capacitor (CC) was remodeled. Initially the cell was developed by Kumar, Masliyah and Sanders (unpublished 2005). It has been discussed in details in Chapter 3. The apparatus was used to determine the dielectric constants of naphtha, bitumen and water-in-bitumen emulsions. The performance of the CC cell was verified initially by using it to measure dielectric constants of four reference liquids: namely, methanol, iso-propanol, toluene and heptane. The comparison between measured values and the reference values from the literature are presented in Table 5.2. The table also includes the results obtained for naphtha, bitumen and emulsion. Measured values of the dielectric constants of the emulsion are discussed in section 5.3.2.

It was not possible to use the CC cell to measure the dielectric constant of water. In the cell water behaved as a conducting liquid. When the CC filled with water was connected to the FLUKE RCL meter, resistance (instead of capacitance) was shown to be

the dominant electric parameter. Moreover, the measured components were outside the measurement range of the basic accuracy limit of the RCL meter. The similar measurements made with methanol differed from the literature value by 30%. For isopropanol, the discrepancy was 10%. The major reason for such discrepancy could be the intrinsic resistive properties (conductance) of such polar liquids.

However, the agreement between experimental results and literature values for non-polar liquids, like toluene and heptane, confirmed that the apparatus could be used for such liquids. Consequently it was used to determine the dielectric constant of naphtha, bitumen and water-in-bitumen emulsions. The experimental results for such measurements are incorporated in tables 4.2 and 5.2.

5.3. PIPE SPOOL CAPACITOR

5.3.1. Dielectric Liquids: Naphtha and Water

The behavior of the composite dielectrics comparable to the flow regimes involved in lubricated pipe flow (LPF) was studied with the Pipe Spool Capacitor (PSC). This study was intended to determine the sensitivity of a capacitance sensor to the presence of fouling oil- and lubricating water-layers of different thickness in LPF. For that purpose, the PSC was designed to measure the corresponding capacitances for different annular arrangements of stationary liquids with distinct boundaries as described in section 3.1.1.2. Naphtha and tap water were selected to imitate the liquids involved in LPF. Naphtha was selected to replicate bitumen because both liquids were found to have a dielectric constant of 2 (see Table 5.2). Moreover, filling and emptying the PSC cell was easy with naphtha but extremely difficult with bitumen.

Table 5.2 Dielectric constants for reference and experimental liquids

Liquid	Dielectric constant (unit)			Ratio (L/E)
	Experiment (E)	Literature (L)	Source	
Methanol	26	33	Buckley et al, 1958	1.3
Iso-propanol	16	18		1.1
Toluene	2	2		1.0
Heptane	2	2		1.0
Naphtha	2	-	Experiment	-
Bitumen	2			
Emulsion	8		Equation (2.6)	
	6-14*			

* Based on the actual range of water volume fractions observed during experimentation.

The mean values of measured capacitances obtained with the PSC cell filled with naphtha and water in various annular configurations are listed in Table 5.3. The COMSOL simulation results are also provided in this table. The full set of results recorded for these tests, including the average and standard deviation of the data, are presented in Appendix 5. For the configurations of naphtha and water in the PSC, negligible standard deviations with respect to the mean values as presented in Appendix 5 confirm the results to be representative and reproducible. In these tables, N:W:N (for example) represents the experimental setup when the outermost, central and innermost gaps (with respect to the electrodes) in the PSC cell were filled with naphtha (N), water (W) and naphtha (N) respectively. Other configurations are similarly denoted. The agreement between measured and predicted (from COMSOL simulations) results is excellent.

Table 5.3 Capacitance of PSC with Naphtha (N) and Water (W)

Liquid Configuration	Capacitance (pF)		Ratio (S/E)
	Simulation (S)	Experiment (E)	
N : N : N	6	6	1.0
N : N : W	7	7	1.0
N : W : N	11	10	1.1
N : W : W	11	10	1.1

As presented in Table 5.3, the measured capacitance with naphtha in three annular shells (N:N:N) was found to be 6 pF. After replacing naphtha in the innermost shell with tap water (N:N:W), the capacitance was found to be 7 pF. The change in capacitance (1pF) for this change in liquids comprising the ‘dielectric medium’ was insignificant. Similarly, capacitance for the N:W:N configuration was 11 pF, which was equal to that for N:W:W, but significantly different from the capacitance for either N:N:N or N:N:W. These results indicate that the measured capacitance is sensitive to the magnitude of the liquid permittivities and the arrangement of the liquids in the cell. This finding implies that a capacitance sensor is likely to lose its sensitivity beyond a certain sensitive zone near the electrodes. Hence, it can be inferred that if a capacitor is applied to lubricated pipe flow the measured capacitance will be influenced mainly by the presence of fouling oil- and lubricating water-layers adjacent to the pipe wall and the lubricated oil core is likely to have no substantial impact on such measurement.

Since it was not possible to quantify this sensitive zone with the PSC cell because its annular gaps are fixed, COMSOL simulations were used. Recall that the good

agreement between the simulation and experimental results (see Table 5.3) suggests that it is reasonable to use COMSOL to evaluate the sensitivity of the capacitance measurement to wall coating thickness. Hence, a capacitance sensor similar to the PSC was simulated with COMSOL. The simulated sensor was considered to consist of a 127mm ID PVC pipe spool with other dimensions exactly identical to the outer most spool of the actual PSC cell. Note that no inner spools were used, i.e. only liquid layers were considered in the simulation. A schematic outline of the simulated pipe spool has been included in Figure 5.1. For this simulation, an annular layer of naphtha ($\epsilon = 2$) was regarded to increase in annular thickness (d) from 0 to 63.5mm at a step of 6.35mm with respect to the inner pipe wall; simultaneously the diameter of a water ($\epsilon = 80$) “cylinder” in the spool was considered to decrease from 127mm to 0mm in steps of 12.7mm. The corresponding capacitance for this simulation scheme have been presented with respect to a dimensionless thickness, $T = d/D$ in Figure 5.1; here d is the increasing thickness of bitumen annulus in the pipe spool. The results indicate that the ratio ($T = d/D$) of the thickness (d) of sensitive zone to the ID of pipe spool is 0.15 (see Figure 5.2). The sensitive zone has been defined as the region beyond which the change in capacitance resulting from a step increase in ‘ d ’ of 6.35mm was 2pF or less. This consideration is based on the fact that the maximum uncertainty observed for measuring capacitance in course of the experiments was ± 1 pF.

The analysis of the sensitive zone thickness presented here is in qualitative agreement with experimental results presented previously in this section and, also, by other researchers. The ratio (similar to T) of the annular thickness of first shell to the ID of outer most spool was about 0.1 and the similar ratio for the combined thickness of first and second shells was 0.25 (see Figure A1.2). These results indicate that such a sensor is capable of identifying the arrangement of liquids, like bitumen and water present within an

annular region next to the electrodes (specifically, during self-lubricated bitumen froth transport). Interestingly, Schaan et al (2002) showed the wall coating of bitumen in LPF could be characterized with a T value of about 0.05. This study involved 50mm and 150mm ID pipes. Moreover, Joseph et al (1999) found the lubricating water to be present within a similar annulus which could be marked with a T value less than 0.05. For this study, the workers used primarily 25mm ID pipe. Though they found the pipe wall to be fouled for LPF, they did not measure the thickness of the oil-layer coating the pipe wall.

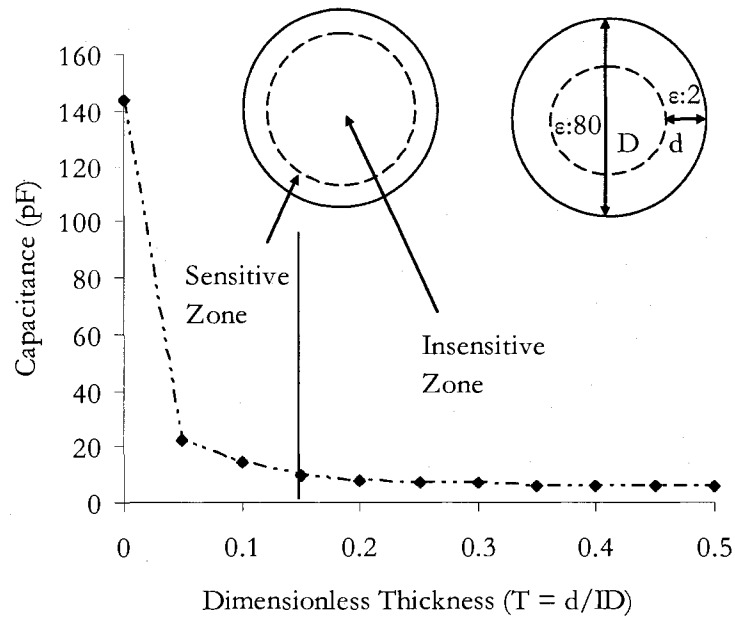


Figure 5.1 Simulation results showing the zone in a pipe over which capacitance measurements will change with wall coating thickness.

On the basis of these studies, it can be reasonably assumed that in LPF both of fouling oil- and lubricating water-layer are present with in a region near the pipe wall, i.e. T

< 0.2 . According to the simulation results of Figure 5.1, a capacitance sensor like the PSC cell is highly sensitive to the liquids present within a similar annulus. Thus, a capacitance sensor similar to the PSC cell can apparently be used to measure the fouling oil layer and lubricating water annulus in LPF.

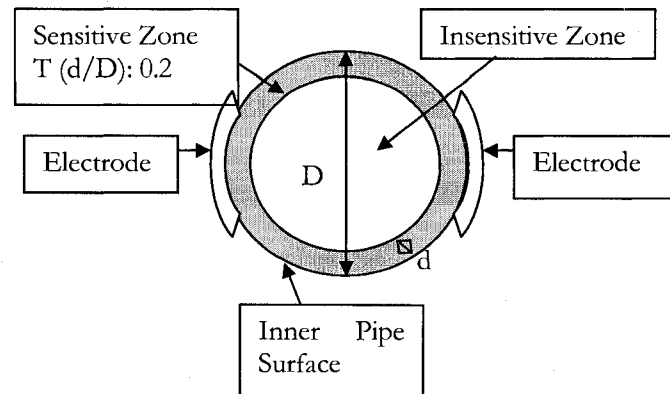


Figure 5.2 Near-wall region where capacitance measurements are sensitive to dielectric changes.

5.3.2. Dielectric Liquids: Emulsion and Water

In this set of measurements, the naphtha was replaced with a stable water-in-bitumen emulsion, which is more representative of the oil involved in lubricated pipe flow (LPF) (see 2.4.3. Emulsion: Dielectric Constant). These experiments were intended to test the sensitivity of pipe spool capacitor (PSC) cell for different annular configurations of emulsion and water. The experimental procedure has been outlined in Chapter 3. The results for this set of experiments, along with the results of corresponding COMSOL simulations, are presented in Table 5.4. For the simulations, the emulsion dielectric

constant was estimated by adding the same of each component weighted with respective to volume fraction (see 2.4.3. Emulsion: Dielectric Constant) and was experimentally measured with the cylindrical capacitor (CC) cell. A full set of results for the configuration of PSC filled with emulsion (E:E:E) is included here as Appendix 6. It should be noted that % water in the emulsion was reduced from 15% to 5% (see Appendix 6) over the course of the experiment. This unexpected loss of water was due to repeatedly transferring the emulsion from one vessel to another (see 3.3.3. Using Emulsion). This variation in water content caused the corresponding emulsion dielectric constant (estimated using equation (2.6)) to change from 6 to 14 (see tables 4.2 and 5.2). This resulted in the predicted capacitance values, as reported in Table 5.4, for E:E:E configuration to vary from 10 pF to 18 pF. Similar explanation is applicable for the theoretical simulation results, as reported in Table 5.4, for other configurations (E:E:W, E:W:E and E:W:W).

However, the uncertainty in emulsion composition changed the capacitance for E:E:E within a small extent (3 pF) (see Appendix 6). Therefore, considering the standard deviation (0.80 pF) as negligible, the average (11 pF) was judged to be representative and repeatable for E:E:E. This result is reported in Table 5.4 as the experimental capacitance. Similar consideration is applicable for other liquid configurations.

Table 5.4 also includes the experimental simulation results obtained from the simulation prepared on the basis of the experimental dielectric constant (8) for the emulsion. For the E:E:E configuration in the PSC cell, this result was 12pF. The theoretical and experimental simulation results for different configurations (namely, E:E:E, E:E:W, E:W:E and E:W:W), as reported in Table 5.4, suggest that the experimental findings are within the theoretical estimates.

The emulsion dielectric constant was determined using the cylindrical capacitor (CC) cell (see 3.3.3. Using Emulsion). The experimental result was within the theoretical estimates (6 – 14) (see tables 4.2 and 5.2) based on the equation (2.6). The variation of theoretical estimate was due to the change in water content of the emulsion. Despite this limitation, the experimental result being within the range of theoretical estimates demonstrated the utility of CC to measure the dielectric constant of a water-in-bitumen emulsion. On the basis of these findings, the dielectric constant of bitumen froth can be measured using a simple capacitance sensor like the CC.

Table 5.4 Experimental and simulation results for PSC with emulsion (E) and water (W)

Liquid-scheme in PSC	Capacitance (pF)		
	Simulation		Experiment
	Theory	Experiment	
E : E : E	10-18	12	11
E : E : W	12-19	14	13
E : W : E	16-23	18	23
E : W : W	17-24	19	22

The comparison of the results obtained for emulsion (Table 5.4) with those for naphtha (Table 5.3) proves that the emulsion behaved as a dielectric with higher relative permittivity than naphtha/bitumen. This suggests a mixture of oil and water will behave as a dielectric if the conducting water phase is not continuous. This finding is in agreement with the study by Erle et al (2000). Such assessment also demonstrates the variation in

capacitance with relative positioning of the dielectrics to be similar for the naphtha – water and emulsion – water systems. Thus, despite the challenges associated with the emulsion water content varying in an uncontrolled fashion, it can be noticed that changes in measured capacitance with emulsion position indicate a capacitance sensor to still be sensitive enough for LPF involving emulsion. These findings also suggest that measuring capacitance for oil - water mixtures (e.g. bitumen froth) involved in LPF will be possible by exposing the electrodes of a capacitance sensor to the composite dielectric medium in the pipeline.

5.4. Parallel Plate Capacitor (PPC)

5.4.1. Dielectric Liquids: Stationary and Flowing Water at Different Temperatures

After the PSC cell experiments showed that measurable changes in capacitance would result from changing the thickness of a near-wall layer of dielectric medium, the flow visualizing Parallel Plate Capacitor (PPC) was used to perform a set of experiments to determine the impact of flow rate and temperature on capacitance measurement. The apparatus was designed with a board of TEFLON over each electrode to shield the plates from the dielectric fluid (see 3.1.1.3 Parallel Plate Capacitor). The cell could be tested with flowing and stationary water and the corresponding capacitance could be measured. Table 5.5 shows the capacitance of PPC at different temperatures measured with respect to various Reynolds numbers (Re) of water flowing through the cell. Almost similar results for stationary and flowing water confirm that capacitance is not a function of flow rate. A negligible standard deviation (0.60 pF) of the data recorded at laminar and turbulent conditions for flowing water justifies: (i) the presentation of average (67 pF) as the representative and repeatable result; and (ii) the claim that capacitance is not a function of

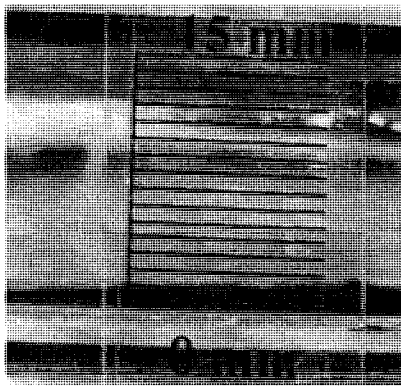
flow rate. On the basis of such findings, the capacitance of a sensor designed for LPF can be inferred to be independent of flow rate. Additionally, there is no theoretical justification for a change in capacitance with flow rate. The negligible change in capacitance over a range of water temperatures from 5°C to 22°C suggests that measurement of capacitance for LPF will not be highly affected by temperature.

Table 5.5: Capacitance of parallel plate capacitor with water flowing at various Reynolds numbers and temperatures

Reynolds number (Re)	Capacitance (pF)			Temperature (°C)
	Record	Average	Standard Deviation	
0	67.1	67.0	0.60	20-22
	67.8			5-7
700	67.4			5
1500	67.4			
1800	67.0			
1900	66.5			
4600	67.3			
4800	66.5			
5200	66.1			
6400	66.8			
7900	68.0			
8000	67.4			
8500	66.1			
9000	66.8			
9300	67.7			

5.4.2. Dielectric Liquids: Bitumen and Water

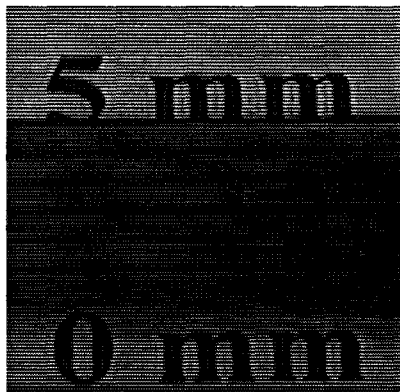
For this batch of experiments, bitumen and tap water were placed in the parallel plate capacitor (PPC) cell to test the dielectric response of the composite medium with varying bitumen layer thickness. This study was conducted to determine the utility of a capacitance sensor to identify the thickness of a coating layer of bitumen on the pipe wall, i.e. wall fouling in lubricated pipe flow (LPF). The results for measuring capacitance with different thicknesses of bitumen placed on the lower plate of the cell have been presented, along with the corresponding simulation results, in Table 5.6. For this set of experiments, stationary water was used. The greatest uncertainty for these tests was involved with measuring the thickness of bitumen layer. The most representative photographs of the average thicknesses of bitumen are shown in Figure 5.3. An error range of $\pm 0.5\text{mm}$ was assigned to the bitumen layer thickness measurements because of the difficulty to prepare a layer of uniform thickness and because of the difficulty in ensuring the camera was perfectly perpendicular to the cell window. In spite of this limitation, the results indicate an appreciable change in measured capacitance with changes in bitumen coating thickness on the lower sensor plate. Again, note the good agreement between the experimental and simulation results, which provided confidence in the experimental findings.



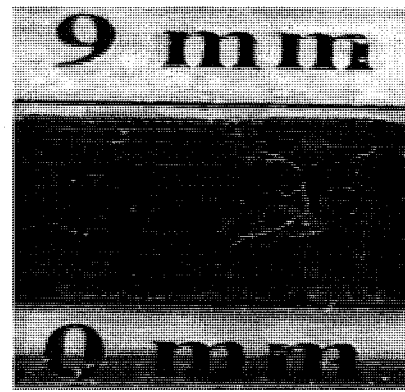
(A)



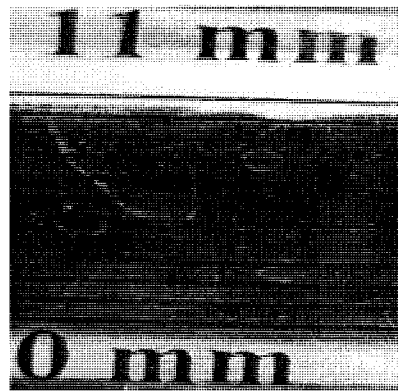
(B)



(C)



(D)



(E)

Figure 5.3 Photographs showing bitumen thickness for stationary tests: (A) 1.5mm, (B) 3.0mm, (C) 5mm, (D) 8.5mm and (E) 10.5mm.

The results presented in Table 5.6 have been depicted in Figure 5.4. In the figure, each capacitance reading represents a combination of bitumen and water in between the electrodes. With prior knowledge of the geometric arrangement of dielectrics (bitumen and

water) in the PPC cell, it is possible to determine the thickness of the bitumen layer from the measured capacitance. This finding suggests that thickness of the oil fouling layer and annular water lubricating layer in LPF can be determined on the basis of measured capacitance if a calibration curve (like Figure 5.3) is available. Again, the excellent agreement between the results of the experiments and the simulations suggests that such static calibration could be based on COMSOL simulation; however, more comprehensive studies are required for that purpose.

Table 5.6 Capacitance of PPC with bitumen layer and stationary water

Thickness of bitumen layer on lower plate (mm)	Capacitance (pF)		
	Experiment (E)	Simulation (S)	Ratio (S/E)
0.0	67	69	1.03
1.5	57	58	1.02
3.0	47	50	1.06
5.0	43	43	1.00
8.5	36	36	1.00
10.5	32	33	1.03

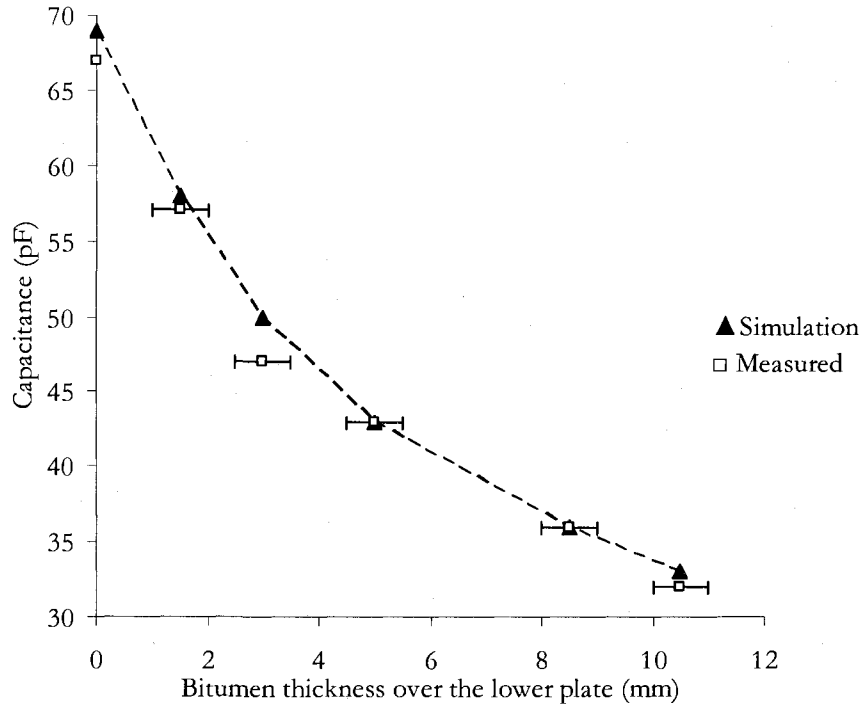


Figure 5.4 Capacitance as a function of bitumen layer thickness in the PPC cell.

For the final experiment, a bitumen layer with an average thickness of 8 mm was prepared on the lower plate of the PPC and the flow rate of water through the cell was set to the maximum value. The flowing water gradually stripped the bitumen coating to finally reduce the thickness of the layer to an average value of 3 mm. Photographs were taken through the viewing window before starting the experiment ($\delta = 8\text{mm}$) and upon completion of the run ($\delta = 3\text{mm}$). Two typical photographs are shown here as Figure 5.5 (A and B). During the experiment, capacitance measurements were recorded at a time interval of one second. The results for this experiment are depicted in Figure 5.6. Clearly, the change in the bitumen layer thickness with time is reflected in the increasing capacitance values. It was not possible to determine the average thickness of bitumen

during the flow condition with visual observation; rather, it was possible to record the changing capacitance. However, on the basis of the previous knowledge about static measurements and simulation results (see Table 5.6 and Figure 5.4), a certain thickness (5 mm) of bitumen on the lower plate could be identified from the recorded capacitance. These measurements clearly indicate that, with proper static calibration, fouling bitumen- and lubricating water-annulus in LPF can be determined using a properly designed capacitance sensor.

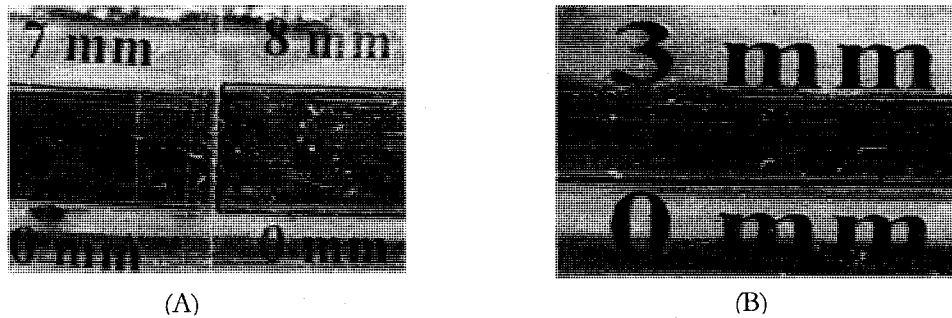


Figure 5.5 Photographs showing the thickness of bitumen layers during flow tests

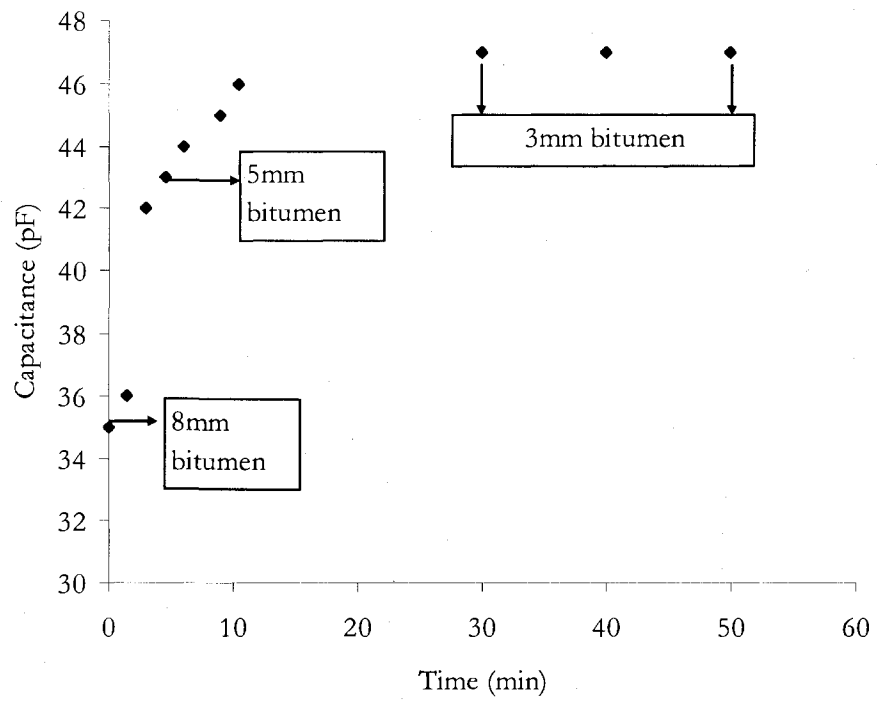


Figure 5.6 Capacitance for changing thickness of bitumen with respect to time

5.5. Summary

The important findings of the present work can be summarized as follows:

- i. The results of the COMSOL simulations matched very closely with experimental results. This provided confidence in the experimental findings. Additionally, it indicates that a commercial capacitance sensor could be calibrated using COMSOL simulations.
- ii. The cylindrical capacitor (CC) cell was used to determine the dielectric constant of non-polar liquids. Hence such a sensor can be used to determine the same parameter for bitumen and heavy oil.
- iii. The cylindrical capacitor (CC) cell was used to determine the dielectric constant of water-in-oil (W/O) emulsion, so the same parameter for the oil-water mixture (e.g. bitumen froth) involved in lubricated pipe flow (LPF) can be measured with a similar sensor.
- iv. Capacitance measurements made with the pipe spool capacitor (PSC) were sensitive to the dielectrics present in the first two annuli and insensitive to the one in the central shell. This finding suggested the existence of a sensitive zone near the electrodes of a capacitor. Such a sensitive zone was predicted with COMSOL simulation. Previous measurements showed that the fouling oil- and lubricating water-layer in lubricated pipe flow (LPF) would be present within the higher sensitive part of this zone. Thus, if employed along a pipeline, a capacitance sensor similar to the PSC will be capable of sensing the wall fouling and/or the lubricating water in LPF.
- v. The pipe spool capacitor (PSC) was successfully used with direct exposure of the electrodes to the liquid medium consisting of naphtha and emulsion. This study

suggests that a capacitance sensor can be used in water lubricated pipeline flows with the electrodes flush-mounted to the pipe wall. Again, the design of the PPC, where the electrodes and process liquids were separated by an insulator, suggests that for a commercial design, it would be possible to place coated electrodes of the capacitance sensor directly on the pipe, thus separating the pipe and the electrodes with an insulator. However, further study is required.

- vi. Capacitance measurements made with the parallel plate capacitor (PPC) were independent of flow rate and temperature. This finding suggests that a capacitance sensor employed for lubricated pipe flow will provide results which will not be affected by variations in mixture flow rate or temperature.
- vii. Capacitance measurements made with the PPC showed significant variation when the thickness of bitumen on the lower sensor plate was changed. This behavior suggests changes of the wall coating thickness in LPF applications could be detected using a capacitance based sensor.

Chapter 6

CONCLUSIONS AND RECOMMENDATIONS

Three capacitance sensors of different geometries were used to test the dielectric behavior of various composite dielectrics. The experimental dielectric media in the bench top apparatus were customized to evaluate the applicability of capacitance sensors for lubricated pipe flow (LPF). Experimental results were verified against the results from simulations produced by using a solver software package, COMSOL Multiphysics 3.3. Based on the experimental and simulation results, the future work required to develop a capacitance sensor for LPF have been suggested.

Experimental results showed that the capacitance of a composite dielectric medium composed of bitumen and water is highly depended on the positions of dielectrics relative to the electrodes of the capacitor. Such sensitivity to the spatial distribution is mainly due to the large difference between the dielectric constants of the two liquids (bitumen and water) and to the geometry of the sensor. Capacitance measurements were mainly influenced by the dielectrics near the electrodes, instead of those located in the central part of the cell. Thus, if a sensor is placed on a water lubricated pipeline, measured capacitance values will be affected by the thickness of the wall fouling and the lubricating water layer; the oil-rich core will have no influence on the measurements. In other words, there is a sensitive zone near the electrodes in such a capacitance sensor. The boundary of the sensitive zone was predicted with COMSOL simulations. The results indicate that for commercial lubricated pipe flows, typical wall fouling layers and lubricating water layers would fall within this zone.

It was shown that capacitance would be independent of temperature and flow rate, meaning that a capacitance sensor, if used for LPF, should give signals that are independent of temperature and flowrate, so that the signal is changing only with changes in wall fouling and/or lubricating water layer thickness.

In the Cylindrical Capacitor (CC) and Pipe Spool Capacitor (PSC), the electrodes were exposed to the dielectric media; however, for the Parallel Plate Capacitor (PPC), layers of an insulator (TEFLON) were used to separate the electrodes from the liquid media. Experiments involving these sensors proved that connection between the electrodes with a conducting liquid (e.g. water) could disrupt the functionality of such apparatus. For Self-Lubricated Flow (SLF) or Continuous Water Assisted (CWA) flow, the lubricating water annulus is separated from the pipe wall by the wall coating layer of bitumen. Thus, the annular water is not likely to hamper the operation of a capacitance sensor with electrodes placed flush with the inner surface of the pipe with SLF and CWA.

The experimental results of the present work were validated with the numerical simulations obtained using COMSOL Multiphysics 3.3a. The COMSOL simulations were conducted because no reasonable analytical expressions were available. Also, the simulations accounted for the impacts of end effects on the predicted capacitance. It is possible that such simulations could be used to design a commercial capacitance sensor for LPF. Moreover, it is likely that COMSOL simulations could also be used for sensor calibration, as described below.

While the present work demonstrates the potential to use capacitance sensors to monitor wall-fouling in LPF, more research is required to develop a commercial capacitance sensor. In this regard, the following work should be done:

- i. **Determining the sensitive zone:** It was experimentally confirmed that sensitivity of a capacitance sensor diminishes quickly beyond a certain distance from the pipe wall. It was not possible to measure this distance with the pipe spool capacitor (PSC). Though the thickness of such sensitive zone was identified with COMSOL simulations, it is necessary to experimentally verify the simulation result. For this purpose, the following steps can be taken:
 - a) A capacitance sensor similar to the PSC cell, but with greater ID, can be built. This cell should be equipped with inner spools separated from one another by not more than an annular distance of 5mm. Thicknesses of these spools should be as small as possible. Dimensions of this cell can be optimized using COMSOL simulations.
 - b) The sensitive zone of a capacitance sensor can also be determined by testing a sensor using a pipe flow loop. In this case, an independent method, like heat transfer measurement (Schaan et al., 2002), would be required so that measurements obtained with the capacitance sensor could be validated.
 - c) A simpler method to measure the sensitive zone would involve a capacitance sensor similar to the PSC cell, but without the inner spools. It should be designed so that it is possible to fix an annular layer of paraffin wax with known thickness and to change this thickness in a controlled manner. After setting up the wax-annulus of a certain thickness, the cell can be filled with water to measure the corresponding capacitance.

- ii. **Sensitivity analysis:** An important area for further study is the sensitivity of a capacitance sensor with electrodes placed on the outside of a commercial steel pipe. For this study, the electrodes can be separated from the pipe with layers of insulating material (e.g. TEFLON). A schematic outline of the proposed sensor is shown in Figure 6.1. This investigation will help to develop a portable capacitance sensor that could be placed over any section of a water lubricated pipeline to quantify the fouling oil layer- and lubricating water annulus-thickness.
- iii. **Optimizing the geometry and dimensions:** It will be necessary to optimize the geometry and dimensions of a commercial capacitance sensor to obtain an optimum signal for LPF applications. This work could be done while testing a capacitance sensor placed on a LPF line. The geometries of the electrodes can be selected based on the studies by Abouelwafa et al. (1980), Gregory et al. (1973) and Nassr et al. (2008). The optimization of the dimensions of the electrodes can be based on COMSOL simulations.
- iv. **Static calibration:** A feasible sensor calibration technique must be developed. This technique must allow for the calibration of the sensor using stationary liquids arranged in a pipe. The liquid placement should be analogous to the flow regimes involved in LPF. It may be possible to base such calibrations on COMSOL simulations; however, this must first be demonstrated.

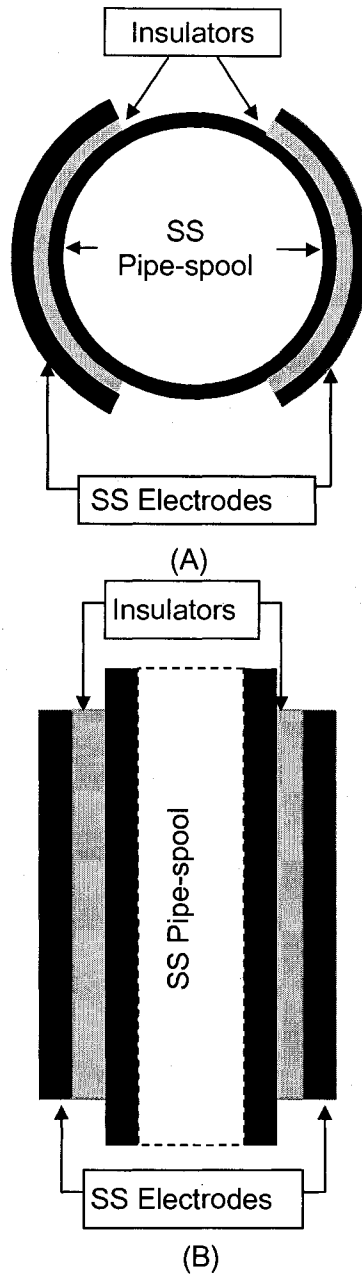


Figure 6.1 Schematic of proposed pipeline capacitance sensor, consisting of stainless steel (SS) electrodes over stainless steel (SS) pipe: (A) Top view and (B) Cut-away side view.

Note: regular carbon steel could also be used.

REFERENCES

- Abouelwafa MSA and Kendall EJM. The use of capacitance sensors for phase percentage determination in multiphase pipelines. *IEEE Transactions on Instrumentation and Measurement*; **IM-29** (1), March 1980, pp. 24-27.
- Abouelwafa MSA and Kendall EJM. Analysis and design of helical capacitance sensors for volume fraction determination. *Review of Scientific Instruments*; **50** (7), July 1979 (a), pp. 872-878.
- Abouelwafa MSA and Kendall EJM. Determination of theoretical capacitance of a concave capacitance sensor. *Review of Scientific Instruments*; **50** (9), September 1979 (b), pp. 1158-1159.
- Arney MS, Ribeiro GS, Guevara E, Bai R and Joseph DD. Cement-lined pipes for water lubricated transport of heavy oil. *Int. J. Multiphase Flow*; **22** (2), 1996, pp. 207-221.
- Baxter and Larry K. Capacitive sensors – design and applications. *IEEE Press Series on Electronics Technology*, John Wiley & Sons, New York, 1997.
- Bensakhria A, Peysson Y and Antonini G. Experimental study of the pipeline lubrication for heavy oil transport. *Oil & Gas Science and Technology – Rev. IFP*; **59** (5) , 2004, pp. 523-533.
- Bello RO. Water-lubricated oil flows in a couette apparatus. M.Sc. Thesis, University of Saskatchewan, January 2004.
- Bezrodnyy MK and Antoshko YU. An acoustic method for measuring the thickness of a flowing liquid film. *Fluid Mechanics Research*; **21** (3), May-June 1992, pp. 1-5.

- Buckley F and Maryott AA. Tables of dielectric dispersion data for pure liquids and dilute solutions. National Bureau of Standards Circular 589; U. S. Dept. of Commerce, Washington, 1958
- Charles ME, Govier GW and Hodgson GW. The horizontal pipeline flow of equal density oil-water mixtures. *The Canadian Journal of Chemical Engineering*; **39**, February, 1961, pp. 27-36.
- Coney MWE. The theory and application of conductance probes for the measurement of liquid film thickness in two-phase flow. *Journal of Physics E (Scientific Instruments)*; **6** (9), September 1973, pp. 903-911.
- Dukler AE and Bergelin OP. Characteristics of flow in falling liquid films. *Chemical Engineering Progress*; **48** (11), November 1952, pp. 557-563.
- Dyakowski T, Hale JM, Jaworski A, White NM, Nowakowski A, Meng G and Rwifa S. Dual-modality probe for characterization of heterogeneous mixtures. *IEEE Sensors Journal*; **5** (2), April 2005, pp. 134-138.
- Erle U, Regier M, Persch C and Schubert H. Dielectric properties of emulsions and suspensions: Mixture equations and measurement comparisons. *The Journal of Microwave Power and Electromagnetic*; **35** (3), 2000, pp. 185-190.
- Gregory GA and Mattar L. An in-situ volume fraction sensor for two-phase flows of non-electrolytes. *Journal of Canadian Petroleum Technology*; **12**, April-June 1973, pp. 48-52.
- Joseph DD, Bai R, Mata C, Sury K and Grant C. Self lubricated transport of bitumen froth. *J. Fluid Mech.*; **386**, 1999, pp. 127-148.
- Joseph DD, Bai R, Chen KP and Renardy YY. Core annular flows. *Annu. Rev. Fluid Mech.*; **29**, 1997, pp. 65-90.

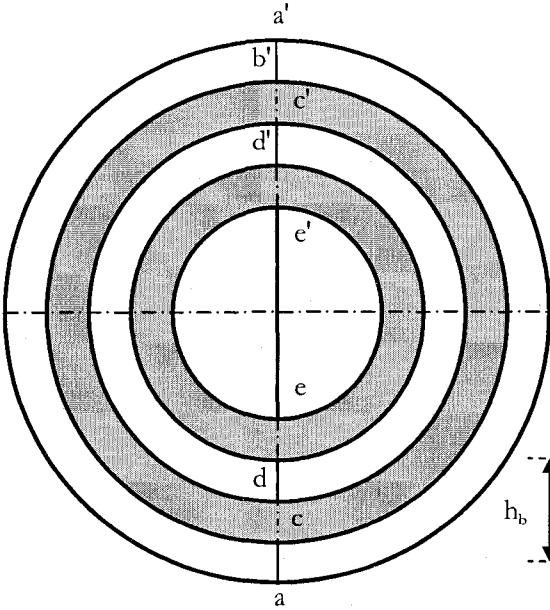
- Joseph DD and Renardy YY; Fundamentals of two fluid dynamics; New York, Springer-Verlag, 1993.
- Jaworski AJ, Dyakowski T and Davies GA. A capacitance probe for interface detection in oil and gas extraction plant. *Measurement Science and Technology*; **10**, 1999, pp. L15-L20.
- Jaworski AJ, Dyakowski T and Davies GA. Application of distributed sensor arrays for monitoring multiphase processes. *Journal of Energy Resources Technology, Transactions of the ASME*; **125**, December 2003, pp. 258-265.
- Kim CH, Lee DW and No HC. Assessment of an ultrasonic sensor and a capacitance probe for measurement of two-phase mixture level. *Journal of Nuclear Science and Technology*; **41** (12), December 2004, pp. 1187-1191.
- Kruka and Vitold R. Method for establishing core-flow in water-in-oil emulsions or dispersions. United States Patent; **4 047 539**, September 13, 1977.
- Lide DR. *CRC Handbook of Chemistry and Physics*. 88th Edition, 2007 - 2008
- McKibben MJ, Gillies RG and Shook CA. A laboratory investigation of horizontal well heavy oil water flows. *The Canadian Journal of Chemical Engineering*; **78**, August, 2000 (a), pp. 743-751.
- McKibben MJ, Gillies RG and Shook CA. Predicting pressure gradients in heavy oil water pipelines. *The Canadian Journal of Chemical Engineering*; **78**, August 2000 (b), pp. 752-756.
- Meng G, Jaworski AJ and Kimber JCS. A multi-electrode capacitance probe for phase detection in oil-water separation processes: design, modeling and validation. *Measurement Science Technology*; **17**, 2006, pp. 881-894.

- Model Library, COMSOL Multiphysics 3.3a; Spherical Capacitor and Tunable MEMS Capacitor.
- Moullin EB. Molecular nature of dielectric. Institution of Electrical Engineers – Journal; **86** (518), February 1940, pp. 113-128.
- Moullin EB. Elementary description of some molecular concepts of structure of dielectrics. Institution of Electrical Engineers – Journal – General; **91** (48), December 1944, pp. 448-455.
- Mouza AA, Vlachos NA, Paras SV and Karabelas AJ. Measurement of liquid film thickness using a laser light absorption method. Experiments in Fluids; **28**, 2000, pp. 355-359.
- Nassr AA, Ahmed WH and El-Dakhakhni WW. Coplanar capacitance sensors for detecting water intrusion in composite structures. Meas. Sci. Technol.; **19**, 2008, 075702 (7pp).
- Neiman O, Sury K, Joseph DD, Bai R and Grant C. United States Patent; **5 988 198**, November 23, 1999.
- Nunez GA, Rivas HJ and Joseph DD. Drive to produce heavy crude prompts variety of transportation methods. Oil & Gas Journal; **96** (43), October 26, 1998, pp. 59-68.
- Ooms G, Segal A, Van Der Wees AJ, Meerhoff R and Oliemans RVA. A theoretical model for core annular flow of a very viscous oil core and a water annulus through a horizontal pipe. International Journal of Multiphase Flow; **10** (1), 1984, pp. 41-60.
- Ooms G and Poesio P. Stationary core-annular flow through a horizontal pipe. Physical Review E; **68** (066301), 2003, pp. 1-7.

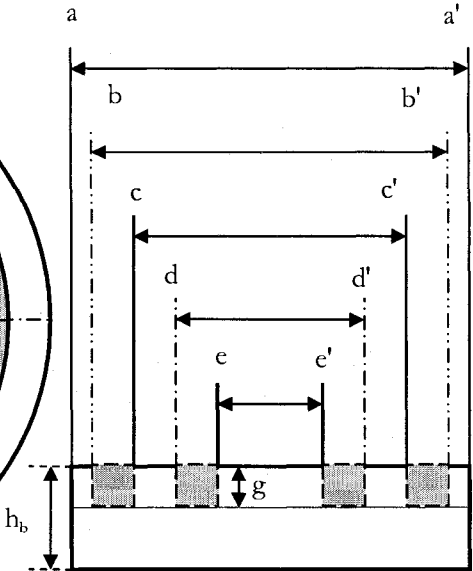
- Ozgu MR, Chen JC and Eberhardt N. A capacitance method for measurement of film thickness in two-phase flow. *Review of Scientific Instrument*; **44** (12), December 1973, pp. 1714-1716.
- Pardo C and Dickau R. Facilities and controls in a heated bitumen pipeline. Proceedings of IPC 2004, International Pipeline Conference; Calgary, Alberta, Canada, October 4 – 8, 2004.
- Perry RH and Green DW. *Perry's chemical engineers' handbook*, 7th Edition. McGraw-Hill, International Editions, Chemical Engineering Series, 1997.
- Russell TWF and Charles ME. The effect of the less viscous liquid in the laminar flow of two immiscible liquids. *The Canadian Journal of Chemical Engineering*; **37**, 1959, pp. 18-25.
- Sanders RS, Ko T, Bai R and Joseph DD. Factors governing friction losses in self lubricated transport of bitumen froth: 1. water release. *The Canadian Journal of Chemical Engineering*; **82**, August 2004, pp. 735-742.
- Sanders RS., *Private Communication*, 2008.
- Saniere A, Henaut I and Argillier JF. Pipeline transportation of heavy oils, a strategic, economic and technological challenge. *Oil & Gas Science and Technology – Rev. IFP*; **59** (5), 2004, pp. 455-466.
- Schaan J, Sanders RS, Litzenberger C, Gillies RG and Shook CA. Measurement of heat transfer coefficients in pipeline flow of Athabasca Bitumen froth. Proc. 3rd Int. Conf. Multiphase Flow, 6-7 June, Banff, Canada BHR Group, Cranfield, UK, 2002, pp. 25-38.
- Sherman P. *Emulsion science*. Academic Press Inc. (London) Ltd, 1968.

- Shook CA, Gillies RG and Sanders RS. Pipeline Hydrotransport with Applications in the Oil Sand Industry. SRC Publication No. 11508-1E02; Saskatchewan Research Council, May 2002.
- Starkovich VS, Bird PF, Dallman JC and Strong RD. Ultrasonic liquid film thickness measurements. Transactions of the American Nuclear Society; **35**, November 1980, pp. 640-641.
- Sun RK, Kolbe WF, Leskovar B and Turko B. Measurement of thickness of thin water film in two-phase flow by capacitance method. IEEE Transactions on Nuclear Science, **NS-29** (1), February 1982, pp. 688-694.
- Strizzolo CN and Converti J. Capacitance sensors for measurement of phase volume fraction in two-phase pipelines. IEEE Transactions on Instrumentation and Measurement; **42** (3), June 1993, pp. 726-729.
- Teyssedou A and Tye P. A capacitive two-phase flow slug detection system. Review of Scientific Instruments; **70** (10), October 1999, pp. 3942-3948.
- Users Manual. Programmable automatic RCL meter, PM 6306, Fluke, Rev. 2, May 1996.
- Yang X and Czarnecki J. The effect of naphtha to bitumen ratio on properties of water in diluted bitumen emulsions. Colloids and Surfaces A: Physicochem. Eng. Aspects; **211**, 2002, pp. 213-222.

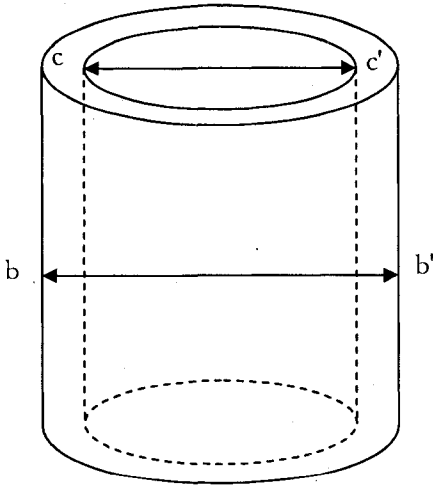
APPENDIX 1: Schematic outlines of experimental capacitance sensors



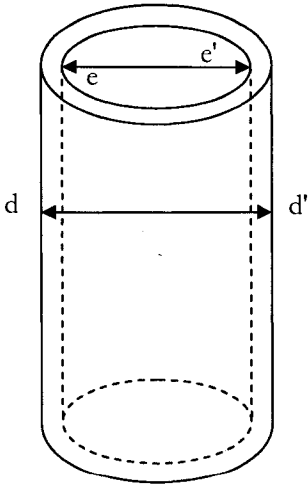
(A)



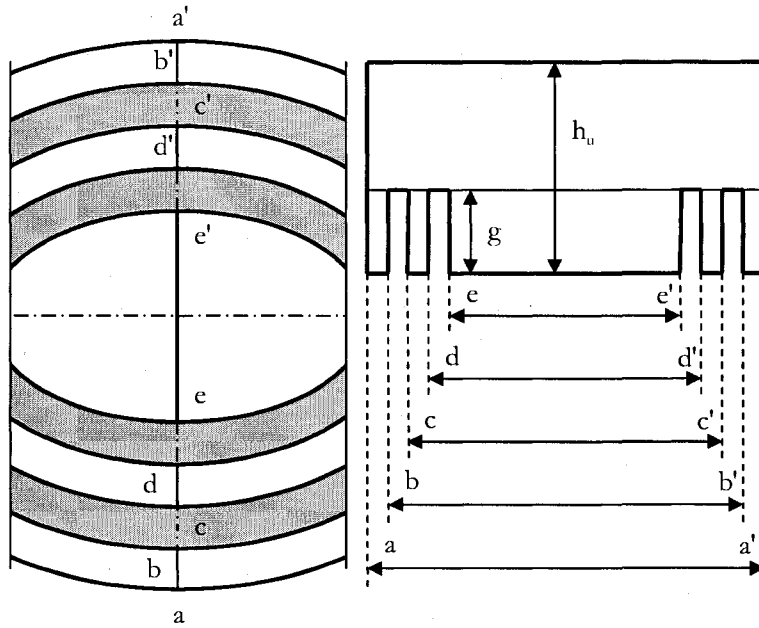
(B)



(C)



(D)



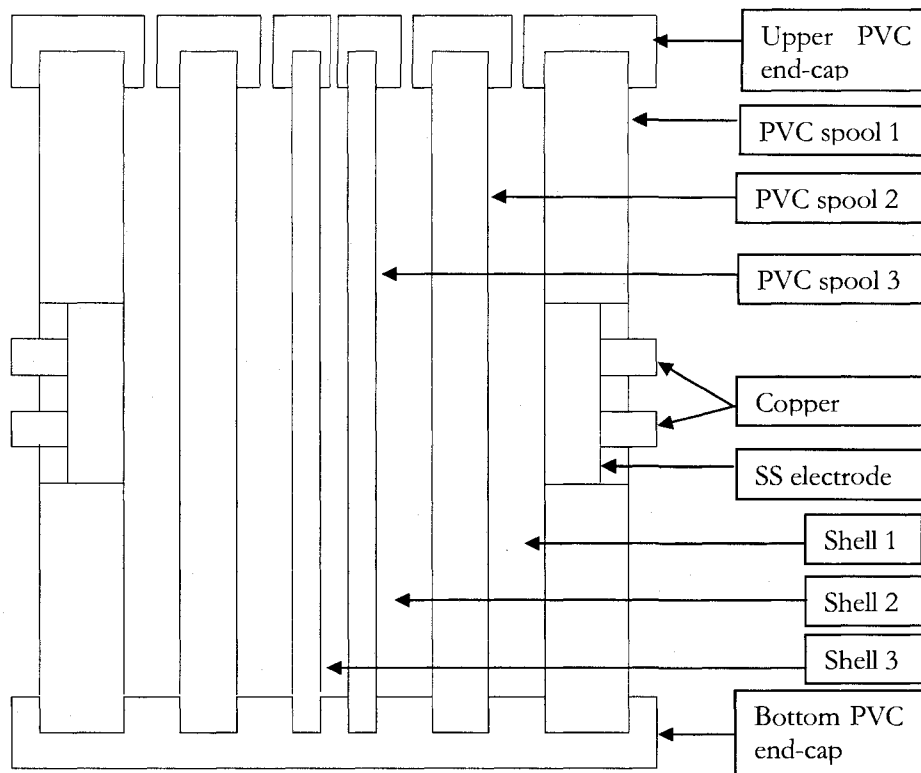
(E)

(F)

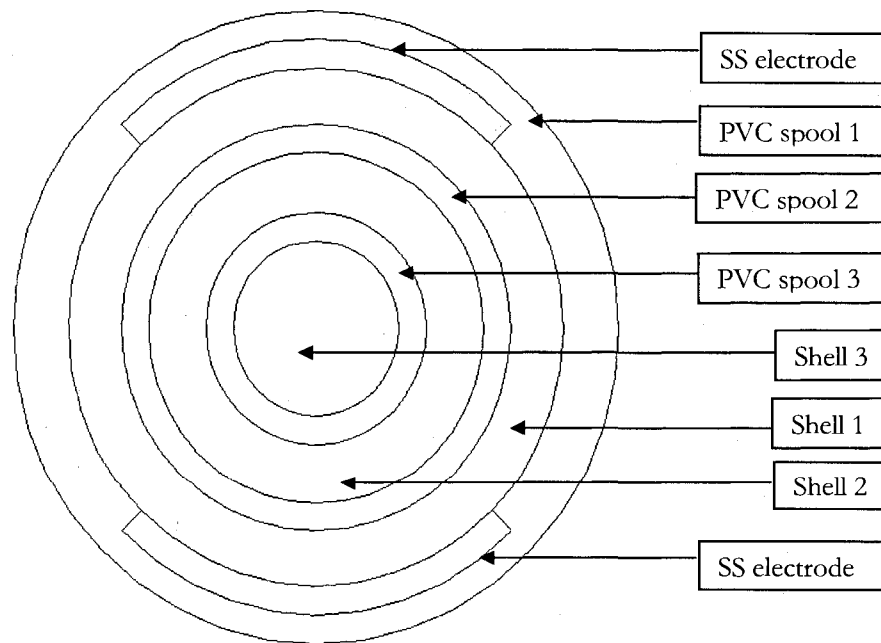
aa': 11.43cm
bb': 10.08cm
cc': 9.17cm
dd': 8.87cm
ee': 8.26cm
g: 0.64cm
h _b : 2.54cm
h _u : 2.06cm

(G)

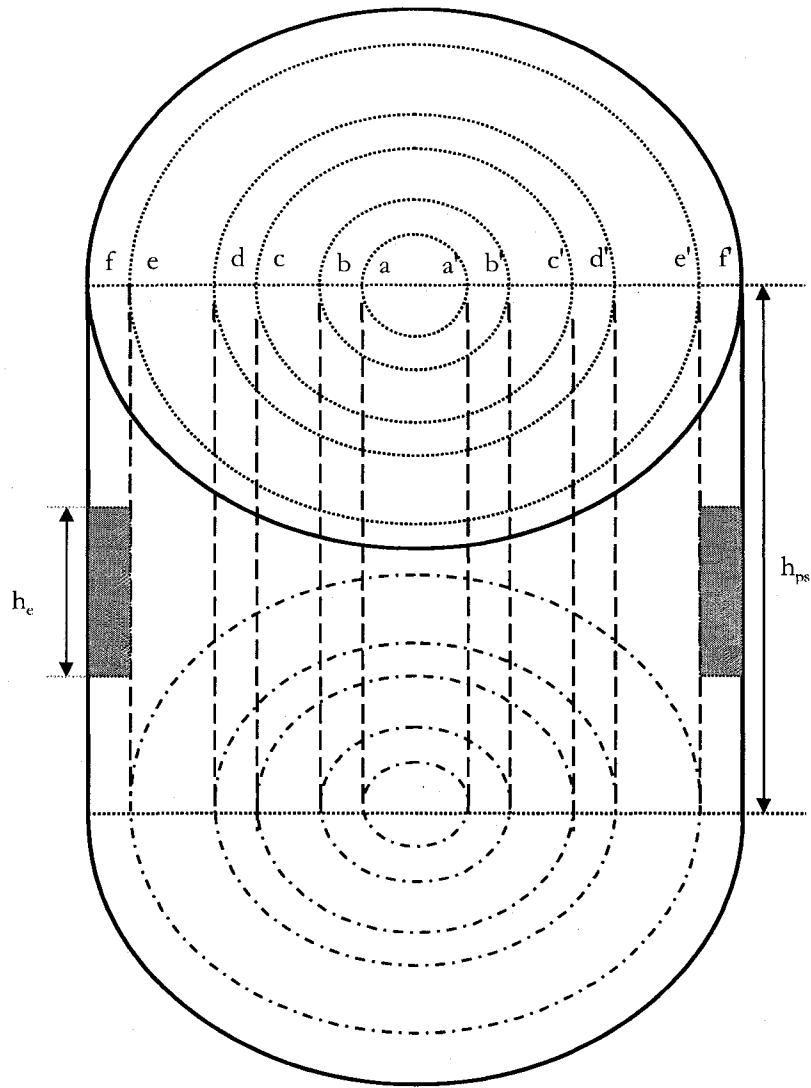
Figure A1.1 Schematic outline of the cylindrical capacitor (CC): (A) top view of bottom end cap, (B) side view of bottom end cap, (C) outer cylinder, (D) inner cylinder, (E) bottom view of upper end cap, (F) side view of upper end cap, (G) dimensions



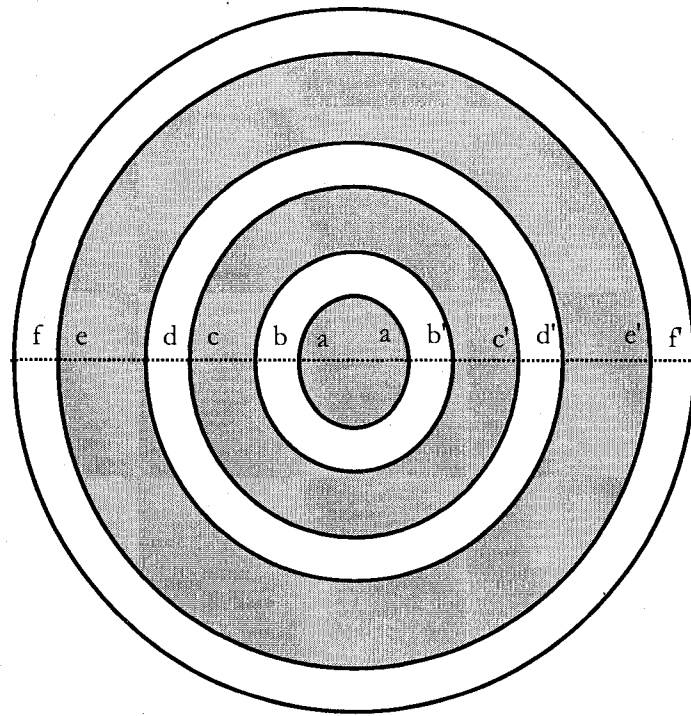
(A)



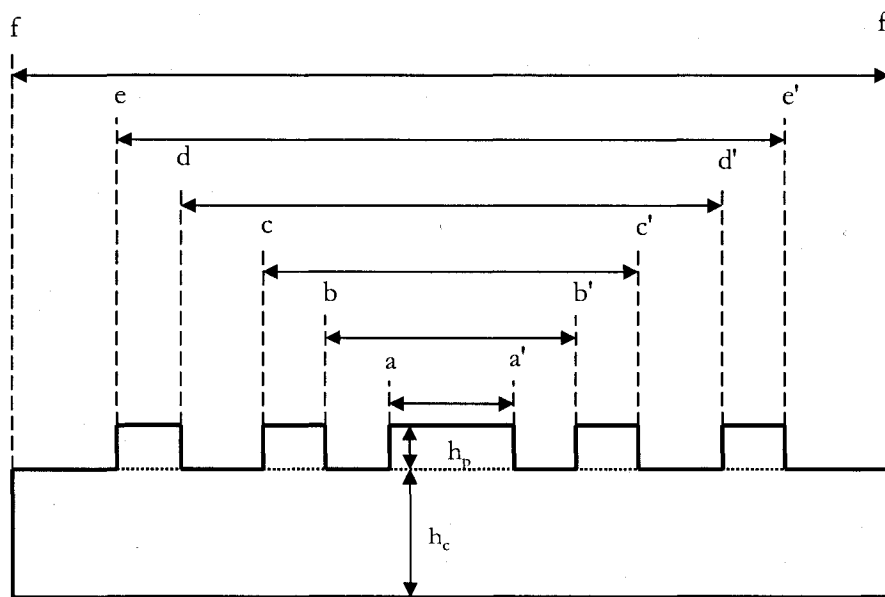
(B)



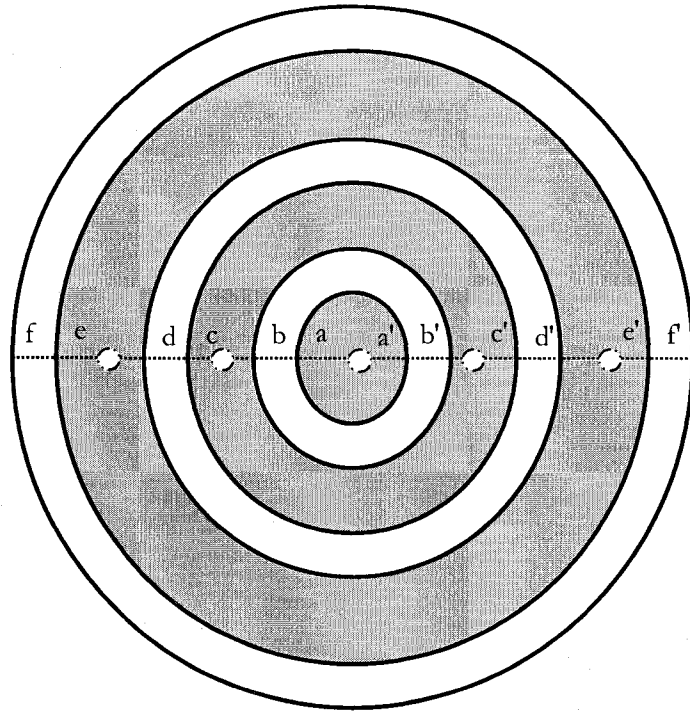
(C)



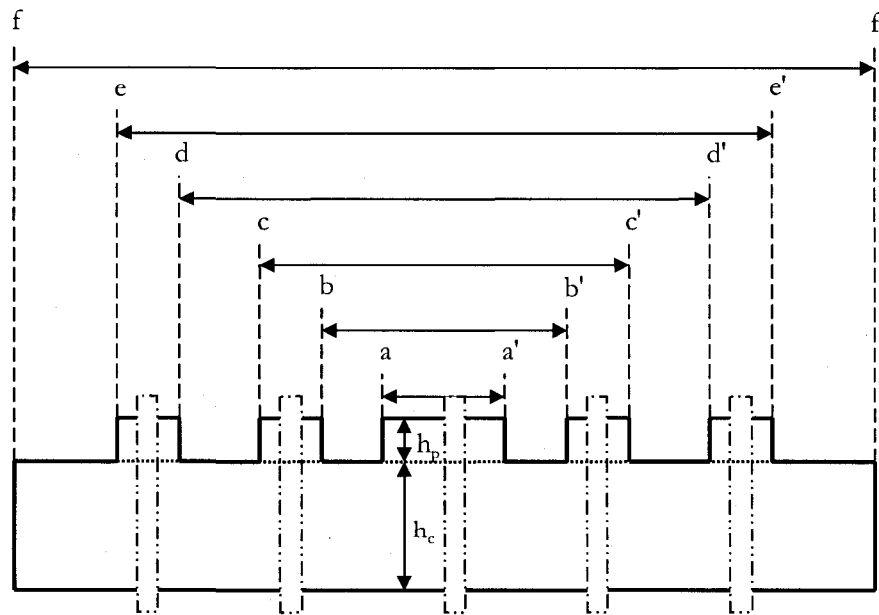
(D)



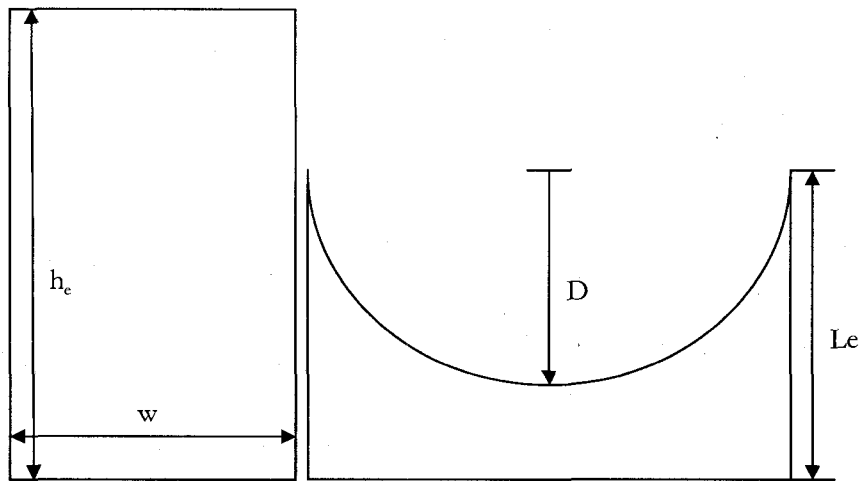
(E)



(F)



(G)



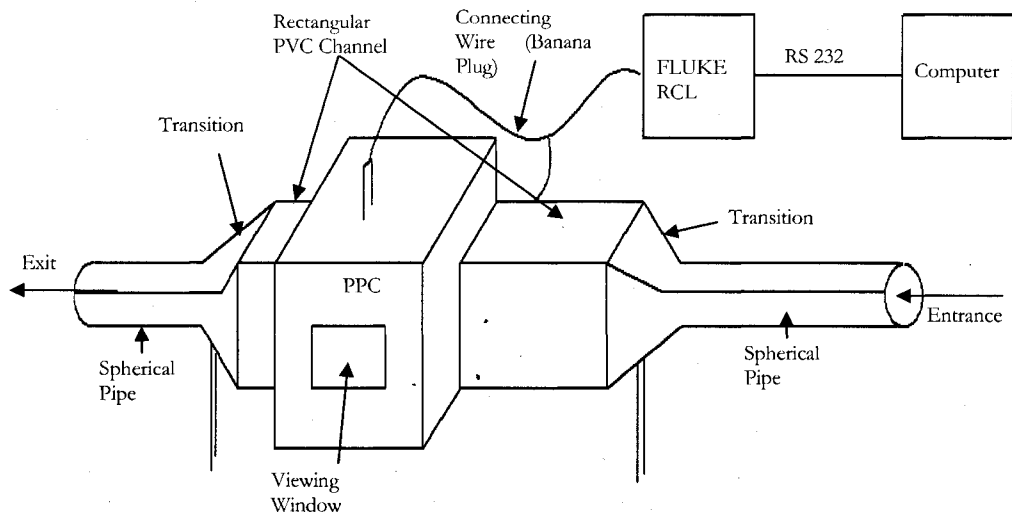
(H)

(I)

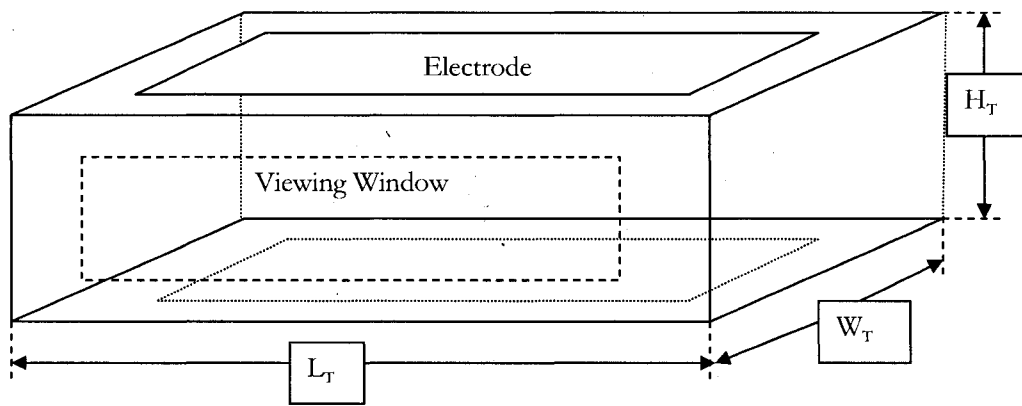
aa': 2.60cm
bb': 3.24cm
cc': 4.48cm
dd': 5.11cm
ee': 6.35cm
ff': 10.16cm
g: 0.79cm
h_{ps} : 31.27cm
h_c : 0.79cm
h_p : 0.40cm
h_c : 15.24cm
w_c : 4.49cm
D_c : 0.93cm
L_c : 1.59cm

(J)

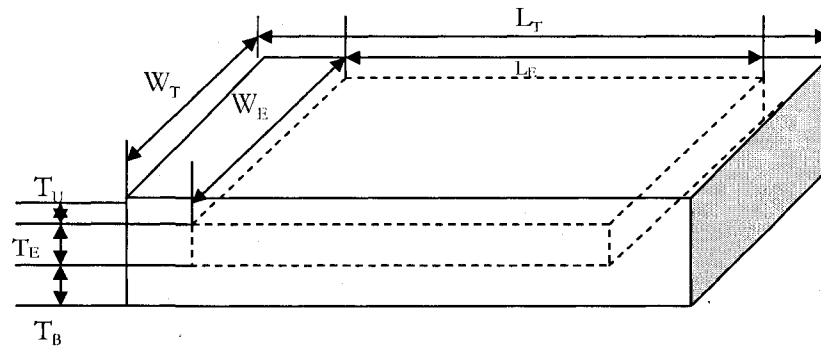
Figure A1.2 Schematic outline of pipe spool capacitor (PSC): (A) cut-away side view of the cell, (B) cut-away upper view of the cell, (C) cut-away view of three concentric pipe spools, (D) top view of lower end cap, (E) cut-away side view of lower end cap, (F) top view of upper end cap, (G) cut-away side view of upper end cap, (H) front view of the 'electrode', (I) top view of the flushed electrode, (J) dimensions



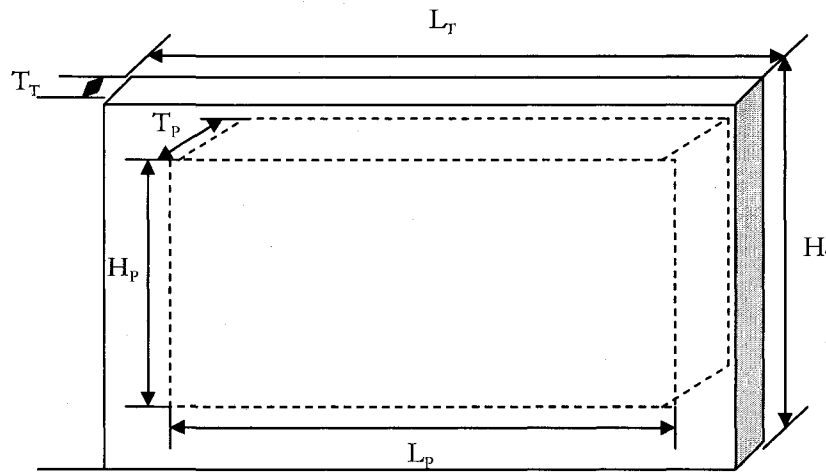
(A)



(B)



(C)



(D)

L_T : W_T : 20.32cm
L_E : W_E : L_P : 15.24cm
T_U : 0.64cm
T_E : 1.43cm
T_B : 0.32cm
T_T : T_P : 0.64cm
H_T : 5.72cm
H_P : 2.22cm

(E)

Figure A1.3 Schematic outline of parallel plate capacitor (PPC): (A) whole set up, (B) the capacitance sensor, (C) upper/lower plate containing electrode, (D) front/rear plate with viewing window, (E) dimensions

APPENDIX 2

Table A2: Specifications for modeling CC cell geometry with COMSOL

Block	Length (m)			Axis base point (m)			Subject
	X	Y	Z	x	y	z	
BLK1	0.1143	0.0762	0.0206375	-0.05715	-0.0381	0.1651	Upper TEFLON cap
Cylinder	Cylinder parameters (m)		Axis base point			Subject	
	Radius	Height	x	y	z		
CYL1	0.05715	0.0254	0	0	0	Lower TEFLON cap (base)	
CYL6	0.05715	0.0206375			0.1651	Upper TEFLON cap and the surrounding air	
CYL2	0.0508	0.1524			0.01905	Outer cylinder	
CYL3	0.045847					Outer cylinder and testing dielectric shell	
CYL4	0.0443865					Inner cylinder	
CYL5	0.041275					Inner cylinder and central hollow	

APPENDIX 3

Table A3: Specifications for modeling geometry with COMSOL for the PPC

Name	Length (m)			Axis base point (m)			Subject
	X	Y	Z	x	y	z	
BLK1	0.1524	0.1524	0.015	0	0	0	Dielectric medium experimental fluid(s)
BLK2	0.1524	0.025			-0.025	0	Plexiglas window
BLK3					0.1524		
BLK4	0.1524		0.005		0	0.015	TEFLON over Plexiglas
BLK5						-0.005	
BLK6					0.1524	0.015	
BLK7					0.1524	-0.005	
BLK8	0.2	0.1524		-0.2	0	-0.005	
BLK9						0.015	PVC channels at input and exit for water flow
BLK10				0.1524		-0.005	
BLK11						0.015	
BLK12		0.01	0.025	-0.2	-0.01	-0.005	
BLK13					0.1524		
BLK14				0.1524	-0.01		
BLK15					0.1524		
BLK16		0.1524	0.015	-0.2	0	0	Dielectric medium in the PVC channel
BLK17				0.1524			

Name	Length (m)			Axis base point (m)			Subject
	X	Y	Z	x	y	z	
BLK18	0.1524	0.15	0.025	0	-0.175	-0.005	Air around the system
BLK19					0.1774		
BLK20	0.2	0.165		-0.2	-0.175		
BLK21					0.1534		
BLK22				0.1524	-0.175		
BLK23					0.1534		
BLK24		0.5024	0.15	-0.2	-0.175	-0.155	
BLK25						0.02	
BLK26				0.1524		-0.155	
BLK27						0.02	
BLK28	0.1524	0.175		0	0	-0.155	
BLK29						0.02	
BLK30					0.1524	-0.155	
BLK31						0.02	
BLK32		0.1524	0.0032		0	-0.0032	
BLK33						0.015	

APPENDIX 4

Table A4: Capacitance of the sensors with air as dielectric fluid

Sensor	Capacitance (pF)			Temperature (°C)
	Record	Average	Standard Deviation	
Cylindrical Capacitor (CC)	287	291	3.5	20 – 22
	288			
	291			
	294			
	295			
Pipe Spool Capacitor (PSC)	3.8	4	0.2	
	3.9			
	4.0			
	4.1			
	4.3			
	4.4			
Parallel Plate Capacitor (PPC)	16.7	17	0.4	
	17.0			
	17.4			

APPENDIX 5

Table A5: Capacitance of pipe spool capacitor filled with Naphtha (N) and Water (W)

Liquid Configuration	Capacitance (pF)			Temperature (°C)
	Record	Average	Standard Deviation	
N:N:W	6.6	6.9	0.3	20 – 22
	6.7			
	6.8			
	7.1			
	7.2			
N:W:N	11.0	11.4	0.4	
	11.1			
	11.2			
	11.3			
	11.7			
	11.9			
N:N:N	5.6	5.8	0.2	
	5.7			
	5.8			
	6.0			
	6.1			
N:W:W	10.9	11.2	0.4	
	11.0			
	11.6			

APPENDIX 6

Table A6: Capacitance of pipe spool capacitor (PSC) filled with emulsion (E:E:E) at room temperature

Capacitance (pF)			Emulsion			
Record	Average	Standard Deviation	Composition		Dielectric Constant	
			Ratio (Naphtha/Bitumen)	% Water	Theory	Expt
9.1	11	0.8	1	5 -15	6-14	8
9.6						
9.9						
10						
10.2						
10.3						
10.4						
10.5						
10.6						
10.8						
10.9						
11						
11.1						
11.2						
11.3						
11.4						
11.6						
11.7						
11.8						
11.9						
12						

APPENDIX 7: Photographs of bitumen with stationary water in parallel plate capacitor

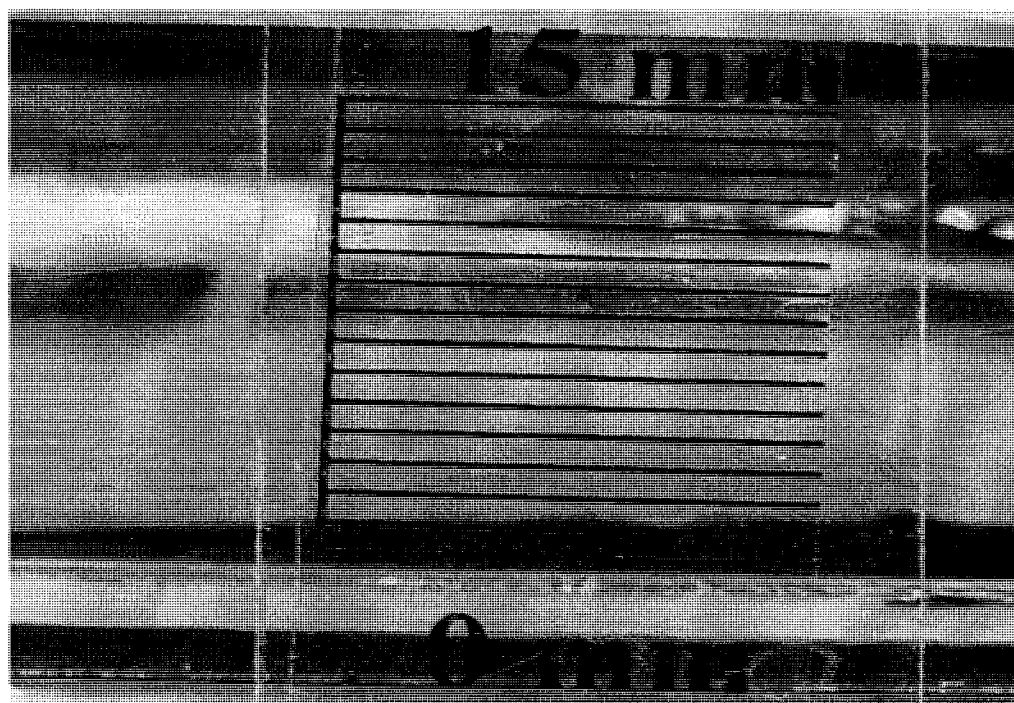
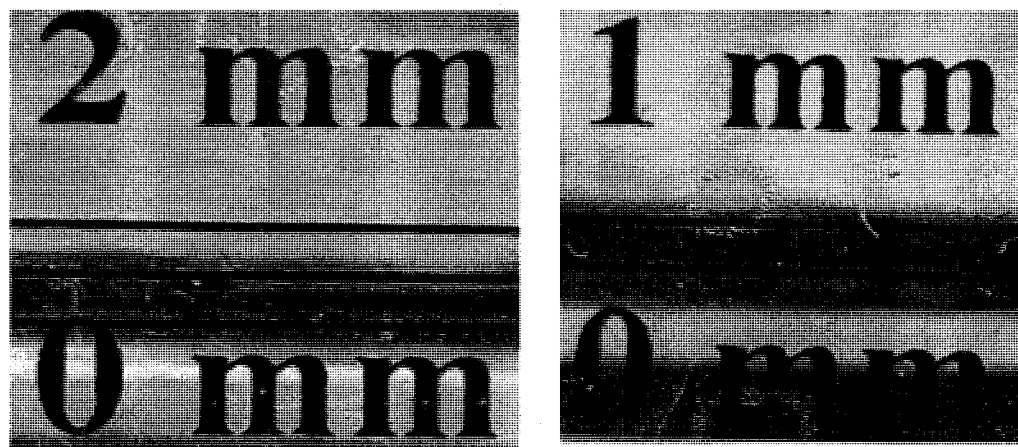
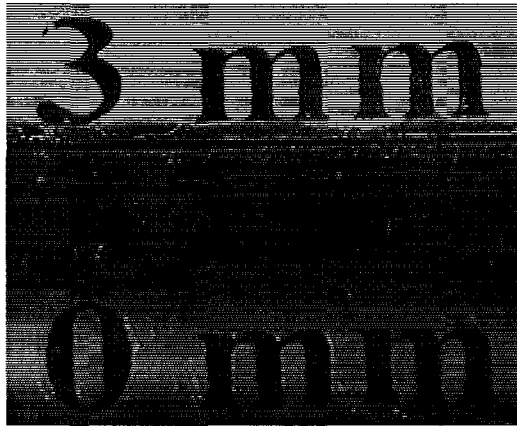


Figure A7.1 Photographs for average bitumen thickness of 1.5 mm



(a)

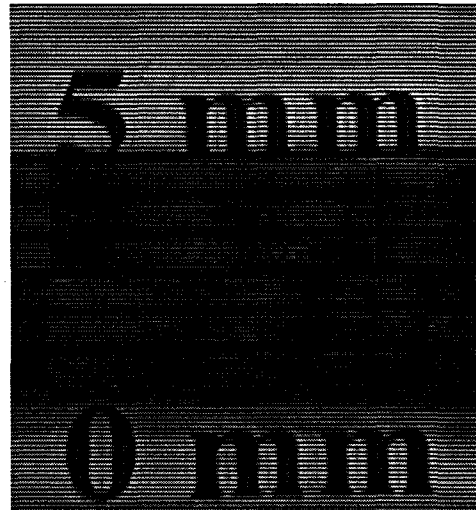


(b)

Figure A7.2 Photographs for average bitumen thickness of 3 mm

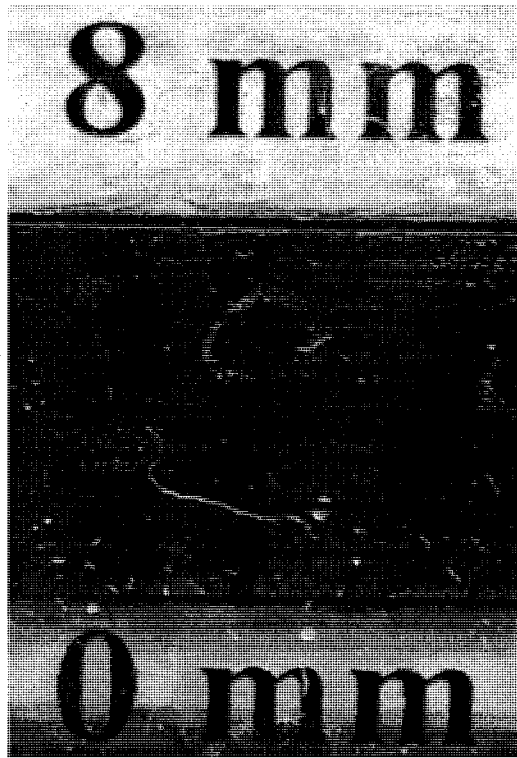


(a)

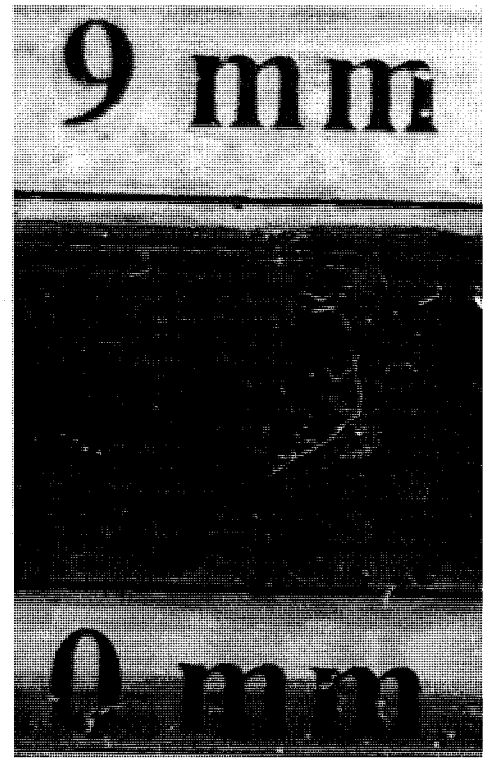


(b)

Figure A7.3 Photographs for average bitumen thickness of 5 mm

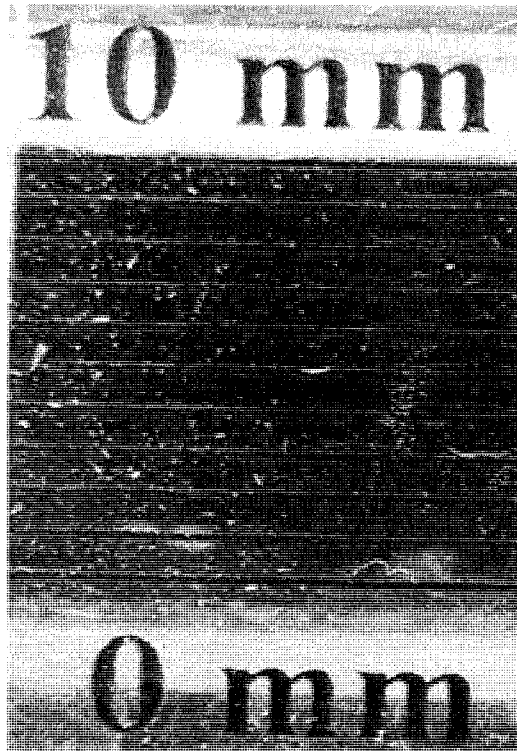


(a)

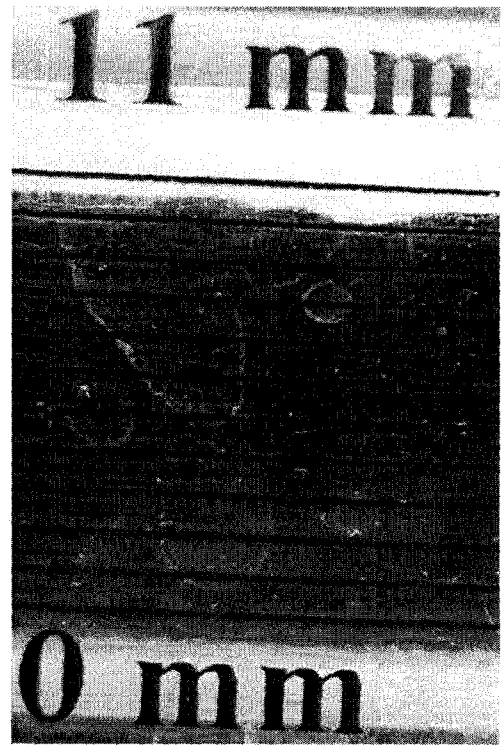


(b)

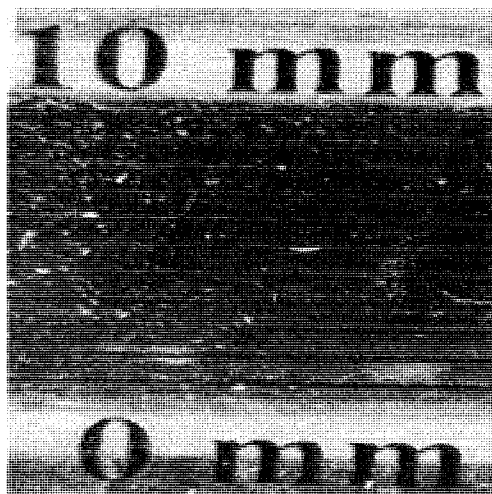
Figure A7.4 Photographs for average bitumen thickness of 8.5 mm



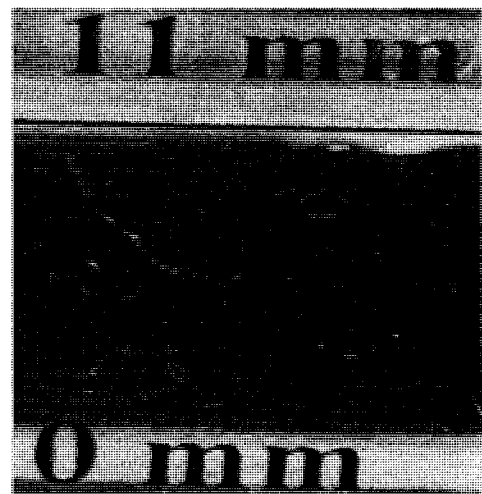
(a)



(b)



(c)



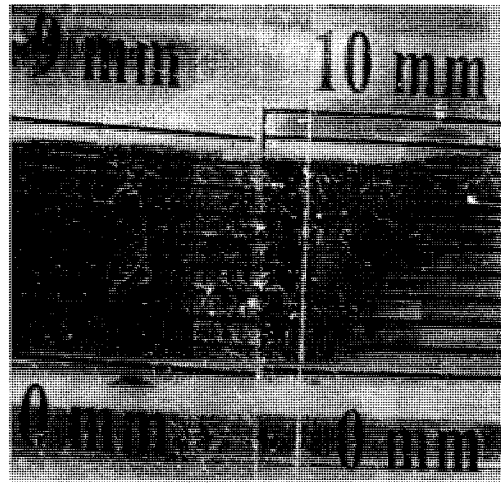
(d)

Figure A7.5 Photographs for average bitumen thickness of 10.5 mm

APPENDIX 8: Photos for the average thicknesses of bitumen in parallel plate capacitor with flowing water



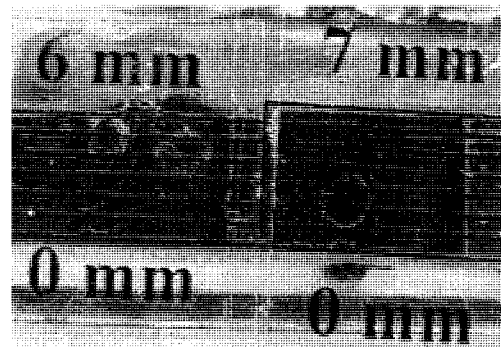
(a)



(b)

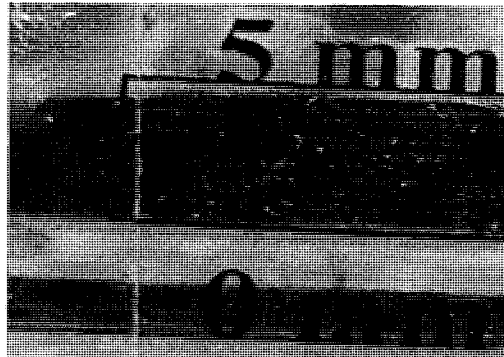


(c)

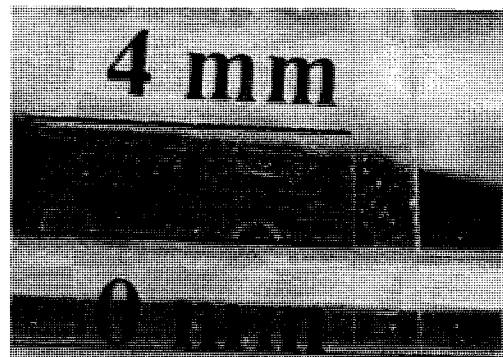


(d)

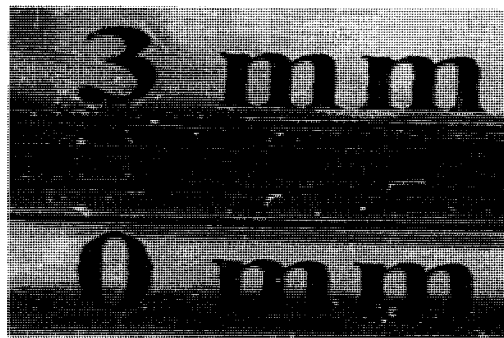
Figure A8.1 Photographs for average bitumen thickness of 8 mm



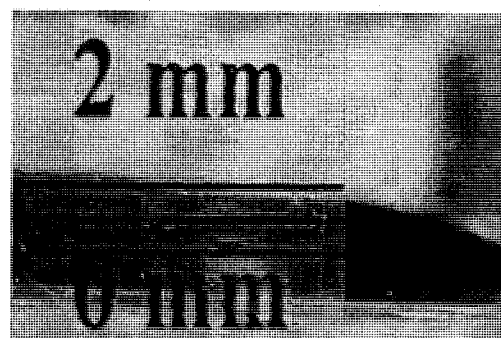
(a)



(b)



(c)



(d)

Figure A8.2 Photographs for average bitumen thickness of 3 mm

APPENDIX 9

Table A9: Capacitance for water flowing over bitumen in parallel plate capacitor

Reynolds # (Re)	Time (min)	Average bitumen thickness (mm)	Capacitance (pF)		Ratio (S/E)
			Experiment (E)	Simulation (S)	
9600	0	8	35	37	1.06
	1.5		36		
	3		42		
	4.5		43		
	6		44		
	9		45		
	10.5		46		
	40		47		
	50	3	47	50	1.06